



Rheology and Thermodynamics of Fat/Oil Blends

Bhagyashri Laxmikant Joshi

Master Thesis

Process Engineering

Advisor: Prof. Dr. Thomas Vilgis and Dr. Birgitta Zielbauer

Advisor: Prof. Dr.-Ing. habil. Reiner Staudt

Mainz, April 28, 2017

Abstract

In this study, the changes in thermal and mechanical properties along with changes in crystal structure of different blends of fats and oil were investigated. Mixtures of Cocoa Butter (CB) with either Tristearin (TS) or Coconut Oil (CO) were used as model system. These fats have been chosen because CB consists of mixtures of Saturated-Unsaturated- Saturated (Sat-U-Sat) kind of triacylglycerols (TAGs) and if this complex system is added to either the easy long chain saturated fat (TS) or the mixed short chained TAGs from CO, then the changes in their physicochemical properties are interesting to observe. Hence to analyze the changes in their properties after blending with each other, four different techniques were used: Differential Scanning Calorimetry (DSC) for the analysis of thermal properties, oscillatory shear rheology for mechanical properties and X-ray Diffraction (XRD) and Polarized Light Microscopy (PLM) for observing the changes in crystal structure and morphology (shape) respectively. The blends were prepared in the ratio of 100% to 0% (weight %) in the step of 10%. For the mixtures of CB with TS following results were obtained. DSC results showed that the crystallization and melting temperature of TS decreased after addition of CB, whereas, in case of CB, both melting and crystallization temperature were almost constant in all mixtures. From XRD results, the calculated spacings suggested that for pure CB and TS polymorphs β_1' (Form IV) in CB and β' in TS has formed, however, specific information for blends could not be obtained as no obvious changes in spacings were observed. PLM showed that TS forms mixture of spherulitic structure and fine mass, whereas CB forms needle like structure along with fine mass (microstructure) and morphology for their blends changes accordingly. Furthermore, rheology results suggested that inter-polymorphic changes occurred during crystallization of CB/TS blend, in addition to a decrease in onset crystallization temperature as a result of adding CB to TS. These results were also supported by DSC results. Tempering was also used for observing the effect or thermal history on crystallization of TAGs in pure CB and TS.

For the mixture of CB with CO, and it was observed that the mixtures of 60% and 70% of CO added to CB behaved as eutectic mixtures. Taking into account all these results it could be shown for the CB and TS blends, TS dominates over CB due to its straight carbon chain, whereas, in the second example CB and CO mixtures might form new molecular

compound. Further experiments are needed to clarify the nature of this compound. Finally, we can conclude here that the molecular interaction strongly depends on the length of TAGs, degree of saturation and induction time for crystallization.

Declaration of Authorship

I declare in lieu of an oath that the Master thesis submitted has been produced by me without illegal help from other persons. I state that all passages which have been taken out of publications of all means or unpublished material either whole or in part, in words or ideas, have been marked as quotations in the relevant passage. I also confirm that the quotes included show the extent of the original quotes and are marked as such. I know that a false declaration will have legal consequences.

Date and Signature

Foreword

This thesis is written as a completion to the master in Process Engineering (MPE) at Offenburg University, Germany. MPE program is mutually organized by Offenburg University and the University of Warmia and Mazury (UWM), Olsztyn, Poland. This program focusses on chemical and thermal process engineering along with biotechnology or food technology. Hence, as a part of MPE, I decided to choose my thesis work in food science. Food science is a huge area of interest now days because of increase in problems related to good food quality such as good taste, texture, storage (shelf life) of food products for longer time etc. This made my interest to research on fundamental properties of lipid systems which will eventually help to increase the food quality as it is used in food application since long time. Therefore, I was in search of such groups that conducts projects related to fundamental research and during this, I came across Prof. Dr. Thomas Vilgis group.

Our group is working on soft matter and food physics at the Max Planck Institute for Polymer Research (MPIP), Mainz, Germany. This institute ranks among top research centers in the field of polymer science worldwide. MPIP was founded in 1983 on the campus of Johannes Gutenberg University, Mainz. This institute offers very strong exposures towards interdisciplinary research projects related to soft materials along with huge number of experimental resources.

Since November, 2016, I have been working on my research under the guidance of Prof. Dr. Thomas Vilgis and Dr. Birgitta Zielbauer. At the beginning I had very little knowledge about this subject and the techniques, used to carry out the experiments, however, I have been able to learn all these in short period of time because of my supervisors support, their valuable insights and proper direction. It was nice to share working bench with them, all the fruitful discussions and learn lots of new ideas and getting to know different working culture in academia. I am happy to be part of this institute and enjoyed a lot working on this research question. I wish that the fundamental research that we carried out during this project would stimulate further detailed investigations in this field.

Table of Contents

<i>Abstract</i>	2
<i>Declaration of Authorship</i>	4
<i>Foreword</i>	5
<i>Table of Contents</i>	6
<i>List of Figures and Illustrations</i>	7
<i>List of Images</i>	9
<i>List of Tables</i>	9
1 Introduction	10
2 Materials and Methods	19
2.1 Materials and general sample preparation.....	19
2.2 Techniques used to carry out the experiments	20
3 Results and Discussion	32
3.1 Analysis of thermal properties of different blends using DSC	32
3.1.1 Blends of Cocoa Butter (CB) and Tristearin (TS).....	32
3.1.2 Blends of Cocoa Butter (CB) and Coconut Oil (CO).....	42
3.1.3 Comparison between blends of CB+TS and CB+CO	47
3.1.4 Phase diagrams for binary mixtures	48
3.2 Molecular structure analysis of CB and TS blends using XRD.....	50
3.3 Study of changes in crystal morphology of CB and TS blends	53
3.4 Analyzing rheological properties of CB and TS during crystallization process	57
3.5 Effect of tempering on polymorph formation	63
3.5.1 Effect of tempering on pure CB	63
3.5.2 Effect of tempering on pure TS	65
4 Conclusion	67
5 Outlook	68
6 References	69

List of Figures and Illustrations:

Figure 1: Schematic for chemical reaction between glycerol and three fatty acids, which produces triacylglyceride (TAG) along with removal of three water molecule (R- represents the carbon chain)	11
Figure 2: The 2D representation of change in FA structure conformation according to the degree of saturation in the carbon chain. Here the number of carbon atoms in each FA is same. (Modified from Vilgis review, 2015).....	11
Figure 3: General representation of one TAG which consists of different FAs. In this TAG, S-represents stearic acid C (18:0), P-Palmitic acid C (16:0) and O is Oleic acid C(18:1).	12
Figure 4: Schematic diagram for concept of crystallization process and steps involved for complete crystallization.....	13
Figure 5: The schematic representation of the basic arrangement of TAG molecules in two different chain length packing structure; (a) one is 2L and (b) another is 3L, where L is the length of one FA (Modified from Vilgis T., 2015).	14
Figure 6: Arrangements of four different polymorphs present in SOS, where S-Stearic acid and O-Oleic acid. The melting temperature changes due to the chain length and angle of tilt.	15
Figure 7: Working Principle of DSC including the general setup (modified from Beccard S.).	20
Figure 8: DSC thermograms for phase change behavior; (a) for crystallization process (exothermic); (b) for melting process (endothermic).	21
Figure 9: Schematic representation of sub cell chain packing structure which is commonly found in TAG polymorphic forms (top view of crystal planes) (Modified from Sato K., 1999).	22
Figure 10: Schematic diagram representing Bragg's law principle.	23
Figure 11: (a) Experimental setup of XRD; (b) Diffractogram (Modified from Gits Magazine).....	24
Figure 12: (a) Principle of PLM; (b) Experimental Setup for PLM	25
Figure 13: Sinusoidal waveforms for torque and displacement.....	27
Figure 14: (a) General experimental setup for parallel plate rheometry; (b) Graphical representation of measured data of sample.	27
Figure 15: Melting endotherm of pure CB and TS along with their respective blends (CB-Cocoa Butter, TS-Tristearin).....	33
Figure 16: Evaluated data from DSC experiment showing the change in melting temperature (determined as a maximum of main peak) with respect to the concentration of TS in the mixture.	34
Figure 17: Representation of solid-solid transition in pure TS.	35
Figure 18: DSC recordings representing the change in polymorphic forms after addition of 10% TS in CB. Form VI was observed after addition of small amount of TS.	36
Figure 19: Crystallization exotherm detected by DSC (CB-Cocoa Butter, TS-Tristearin). ...	37
Figure 20: (a) Comparison of crystallization Temperature (CT) for CB and TS; (b) ΔH of crystallization vs. concentration of CB and TS.....	38

Figure 21: Re-melting Endotherm of pure CB and TS along with their blends (CB-Cocoa Butter, TS-Tristearin).....	40
Figure 22: Melting segment of Cocoa Butter indicating the presence of different polymorphs in the mixture.	40
Figure 23: (a) Comparison of melting Temperature (MT) for CB and TS; (b) ΔH of fusion vs. concentration of CB and TS.	41
Figure 24: DSC endotherm for the mixtures of CB and CO.....	43
Figure 25: DSC exotherms for the mixture of CO and CB and their comparison with individual fat.	45
Figure 26: DSC endotherm for CO and CB and their respective blends in between.....	45
Figure 27: Data evaluation from DSC endotherm in terms of change in melting temperature of Coconut Oil and Cocoa Butter in their respective blends.....	47
Figure 28: (a) Phase diagram constructed from calorimetry data of CB (POP/POS/SOS) and TS (SSS) blend; (b) Phase diagram for mixture of POP and PPP (Bruin, 1999).....	49
Figure 29: Phase diagram plotted from DSC data (considering melting temperature and weight fraction of coconut oil as a basis) of CB (POP/POS/SOS) and CO (LaLaLa/CLaLa/CCLa/LaMM) mixture.....	50
Figure 30: XRD reflexes for CB and TS and comparison with their blends.....	51
Figure 31: Schematic representation of possible interaction between metastable polymorph of both TS and CB (POP).	52
Figure 32: Difference in crystal morphology in case of blends of CB/TS with respect to their concentration in the mixture. The samples are as- (a) Pure TS, (b) TS (90%) +CB (10%), (c) TS (80%) +CB (20%), (d) TS (70%) +CB (30%), (e) TS (60%) +CB (40%), (f) TS (50%) +CB (50%), (g) TS (40%) +CB (60%), (h) TS (30%) +CB (70%), (i) TS (20%) +CB (80%), (j) TS (10%) +CB (90%), (k) Pure CB; (CB- Cocoa Butter; TS-Tristearin; with scale bar of 32 μ m).	57
Figure 33: (a) Schematic representation of crystallization of fats during rheology (b) Co-relation between the schematic and one result from rheology.....	58
Figure 34: Graphical representation of moduli vs. temperature in which the changes in moduli after addition of CB in TS during crystallization process is shown.(G'–Storage Modulus, G''-Loss modulus; CB-Cocoa Butter, TS- Tristearin).....	60
Figure 35: Co-relation between rheology and DSC result for pure TS sample to understand the change in viscoelastic properties during crystallization process.....	60
Figure 36: Co-relation between rheology and DSC result for pure CB sample to understand the change in viscoelastic properties during crystallization process.....	62
Figure 37: Graphical representation of change in crystallization temperature during rheology experiment.....	62
Figure 38: Comparison of polymorphism in tempered and non-tempered CB; (CB_tempered_#1- 60 °C for 15 hours, 30°C for 2 hours, 26 °C for 1 hour, 32°C for 2hours; 'CB_tempered_with stirring', with same parameter as in CB_tempered_#1 along with 350 rpm speed).	65
Figure 39: Comparison of polymorphism in tempered and non-tempered TS; (CB_tempered_#1- 60 °C for 15 hours, 30°C for 2 hours, 26 °C for 1 hour, 32°C for 2hours)	66

List of Images:

Image 1: Marktubes used as a sample holder to carry out measurements in XRD.	24
Image 2: (a) HR-3 Rheometer; (b) Thermal insulator for controlling the temperature gradient	28
Image 3: The path for melting of crystals in the mixture of TS (40%) + CB (60%).	54

List of Tables:

Table 1: Different polymorphic forms of CB and their respective melting temperature	17
Table 2: The ratio of amount of fat/oil in blends preparation	19
Table 3: Three segments for measurement in DSC.....	22
Table 4: Three segments for measurement in PLM	26
Table 5: Experimental parameters for rheology	29
Table 6: Steps used for tempering process in climate chamber	30
Table 7: Fusion enthalpies of TAG polymorphs in CB.....	42
Table 8: Effect on CB after addition of TS (saturated fat) and CO (mixed saturated short chained TAGs)	47
Table 9: Comparison between the calculated spacings of CB and TS with literature values (vs-very strong; s-strong)	51

Chapter 1

Introduction

“The kitchen is a laboratory, and everything that happens there has to do with science. It is biology, chemistry, physics. Yes, there is history. Yes, there is artistry. Yes, to all of that. But what happened there, what actually happens to the food is all science” (Alten Brown). So, food science is the study of the nature of food, the chemical structure of food components, interaction between them, changes in their structure over the environmental conditions and hence these factors are lead to the quality of food products, which should have long shelf life and good nutritional values so that they ultimately add on to healthy life of human as well as animals. One of the important studies in food science is the physics involved in food. Food physics is the study of observing the physicochemical properties of components of food, which is important for developing optimized solution for food production processes. In our study, we have focused on fats and oils i.e. lipid system, as they have been used as a raw material since very long time not only in food applications but also in other applications such as some oils used as a part of lubricants in automobile industries, some fats are used as a coating material in pharmaceutical sector. Therefore, in food oriented application fats and oils play an essential role to add unique properties such as flavor, good texture, lubricity and satiety to foods. However, the resources for producing good quality fats and oils are very expensive due to increase in population and simultaneously their requirements. Hence, to overcome such problem, the blending of different oils or fats becomes very interesting topic to study. Also, blending can result in formation of new product which shows the changes in physical and chemical properties and this can indeed help to solve the problems involved with pure fat and oil such as rancidity, oxidation, viscosity etc. For instance sesame oil possesses antioxidant properties but it does not have good sensory characteristics therefore it is not good for deep frying. If this oil mixed with palm olein it provides the crispness, aroma and flavor to the food (Abdulkarim et al., 2010).

The terms fats and oils are used interchangeably, as they are usually based on their physical state of the material at ambient temperature and tradition. Generally, fats appear solid at ambient temperatures and oils appear liquid (O’Brien R., 2009). However, the chemical composition defines the characteristics of the individual fat or oil, which eventually determines the suitability of such ingredients in different applications. Fats and oils are the esters of three fatty acid chains; they are called triacylglycerol or triglycerides (TAG). It is a

chemical reaction between one glycerol molecule and three fatty acid (FA) chains. The schematic of the reaction is shown in Figure 1, in which R represents the long chain of carbon atoms. These FAs contain at least 4 carbon atoms and depending on their carbon chain length the physical behavior of oils and fats changes (Vilgis T., 2015). Another parameter to be considered is the degree of saturation, which describes the presence of double bonds between two carbon atoms. Therefore, according to degree of saturation, FAs are distributed typically in two types, one is saturated (with no double bond) and another is unsaturated (at least one (cis) double bond). The general representation of FA is in the form of C(n:s), where, n represents the number of carbon atoms present and s is the degree of saturation i.e. number of carbon-carbon (C-C) double bonds.

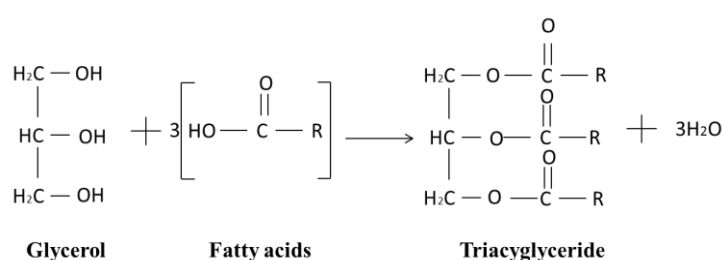


Figure 1: Schematic for chemical reaction between glycerol and three fatty acids, which produces triacylglyceride (TAG) along with removal of three water molecule (R-represents the carbon chain).

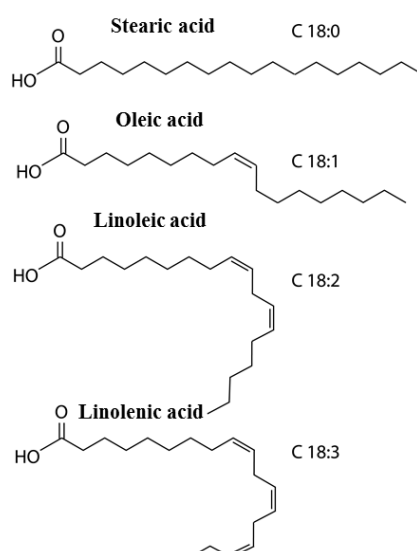


Figure 2: The 2D representation of change in FA structure conformation according to the degree of saturation in the carbon chain. Here the number of carbon atoms in each FA is same. (Modified from Vilgis, 2015).

In Figure 2, it is shown how the conformation of FAs changes depending on number of double bonds present in the carbon chain. They all contain the same number of carbon atom C (18), but their degree of saturation is increasing from stearic acid to linolenic acid respectively, and so the structure becomes more complex than that of the saturated acid (stearic acid). Hence, during crystallization process, stearic acid has the advantage of packing itself densely due to its straight chain. This helps to form a crystalline structure with smaller amount of defects (almost perfectly arranged crystal structure) and so during melting of these crystals the energy required would be higher as compared to the crystals with more defects. Therefore, due to fewer defects in crystal structure, it becomes more stable and eventually, melts at very high temperature. As the degree of saturation increases the kinks start to form, which creates difficulty in forming a closely packed structure during crystallization. Therefore, the improper crystal structure formation occurs, which leads to less stability and hence it melts at lower temperature. Thus, the melting temperature decreases from stearic acid to linolenic acid (74 °C to -16.5 °C) (Vilgis T., 2015). In Figure 3, the representation of one TAG is shown. TAGs are named according to FA position during esterification. In Figure 3, A FA composed of POP is shown as an example. Here, P represents palmitic acid and it is situated at 1st position, O-Oleic acid, which is at 2nd position and S-Stearic acid, this attached to 3rd position to the glycerin part.

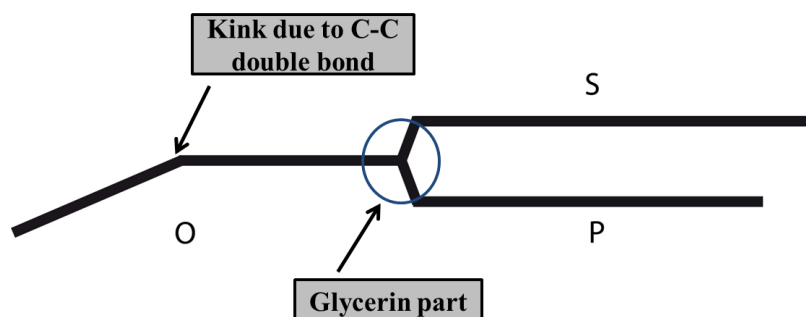


Figure 3: General representation of one TAG which consists of different FAs. In this TAG, S-represents stearic acid C (18:0), P-Palmitic acid C (16:0) and O is Oleic acid C(18:1).

In general fats and oils contain mixtures of different TAGs and this makes the study of crystallization of such fats and oils very interesting. The production of good quality food product depends not only on the initial processing in factory but also to the storage conditions e.g. in warehouses, shop or home (Himawan et al., 2006). Hence to understand the concept of

crystallization in TAGs, firstly, it is important to acquire the knowledge of the crystallization process. Two main steps are involved in crystallization process, which are as- nucleation and crystal growth (Figure 4). Nucleation is the process of phase change in which crystal formation takes place from liquid and this nucleation process is further distributed in two sub categories as- primary nucleation and secondary nucleation. Primary nucleation refers to the birth of very small bodies of a new phase within the existing phase. This primary nucleation could be either homogeneous or heterogeneous depending upon the operational situations such as if nucleation process is occurring due to presence of catalyze (heterogeneous nucleation), then it would be faster compared to the one without catalyze (homogeneous nucleation) (McCabe, W.L., 2005). After formation of the 1st solid crystals, the nuclei of other crystals starts to form according to the earlier crystal formation, so in this case, the previously formed crystals act as a seed for next crystal formation. Later, the crystal growth takes place, which consists of arrangement of these molecules or atoms in a specified crystal lattice and the packing of this lattice defines the stability of the crystals. Therefore, the crystal stability is dependent on how the 1st crystals are forming and on the rate of crystal growth.

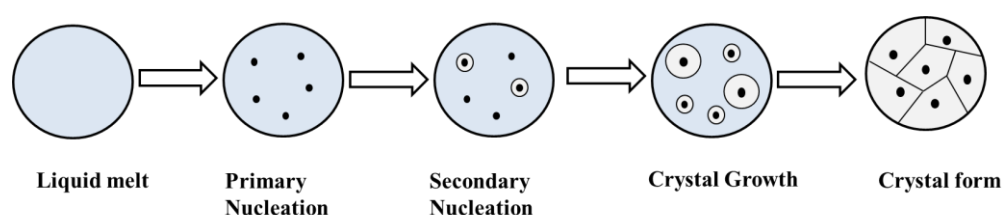


Figure 3: Schematic diagram for concept of crystallization process and steps involved for complete crystallization.

Now, in case of TAGs, the molecules can crystallize in different forms which are called as polymorphs. Each polymorph has specific lattice structure and depending on their packing ability (loosely packed or densely packed) the melting temperature changes.

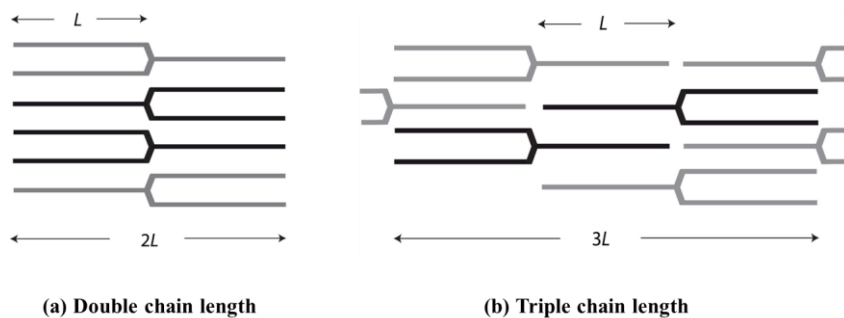


Figure 4: The schematic representation of the basic arrangement of TAG molecules in two different chain length packing structure; (a) one is $2L$ and (b) another is $3L$, where L is the length of one FA (Modified from Vilgis T., 2015).

In Figure 5, the arrangement of the TAG molecules after crystallization process is shown. The stacking of different TAGs is possibly done by two ways (basic structures), one is double chain length and another is triple chain length. And triple chain length structure is the stable as compared to double chain length as it is more closely packed than double chain length structure. Hence, generally, the melting temperature is higher for the polymorphs with the triple chain length arrangement. Basically there are three main polymorphs present, which are as α , β' , β and their stability is dependent on their stacking arrangement. Whereas, the exact types of polymorphs formation depends on TAG composition as well as the process used for crystallization. For instance, in case of SOS (Stearate-Oleate-Stearate), 4 different types of polymorphs exist depending on the crystallization conditions. They differ with respect to their chain length (double or triple) and the angle between the methyl plane and TAG (shown in Figure 6). In α polymorph the arrangement of TAGs is of double chain length packing (hexagonal structure) with no angle of tilt, whereas in γ , the double chain length increased to $3L$, therefore it is more closely packed, and this leads to higher melting point than α . Another parameter is the angle of tilt, in the β' polymorph (orthorhombic structure) there is slight decrease in angle and therefore the chain length is decreased to some extent. Due to tilt, they form closer packing than γ polymorph and hence the melting temperature increased by one degree. In case of β_1 and β_2 (triclinic structure), the angle decreased to approx. 50° to 70° and because of this decrease in angle, they pack tightly together and hence it melts at higher temperature than other polymorphs (Himawan et al., 2006, Vilgis T. 2015).

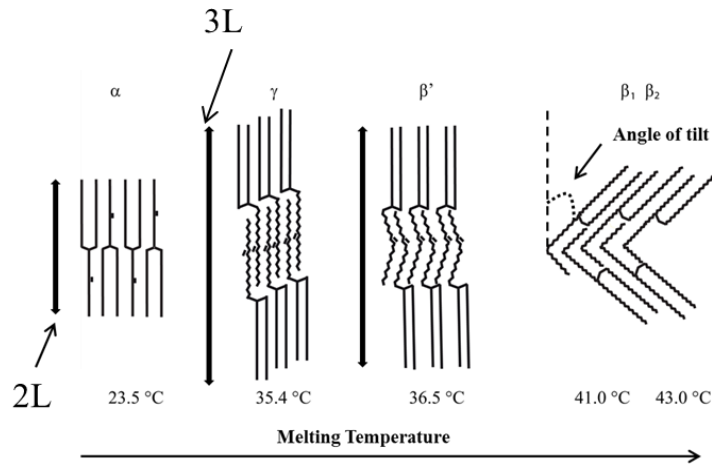


Figure 5: Arrangements of four different polymorphs present in SOS, where S-Stearic acid and O-Oleic acid. The melting temperature changes due to the chain length and angle of tilt.

Furthermore, the energy involved in crystallization and melting of these polymorphs is measured as a term enthalpy change. Therefore, thermodynamics plays an important role during crystallization and melting of TAGs (fats and oils). The stability of individual polymorph and driving force required for transformation between the two or more polymorph is investigated by their Gibbs free energy (G). The Gibbs free energy is described as the relation between enthalpy and entropy at particular (constant) temperature. It is shown in equation below (Nguyen, T.K., 2009)

$$G = H - TS$$

Where, G-Gibbs free energy, H-Enthalpy, T- Temperature and S- Entropy.

During melting process, the entropy of the system increases due to randomization of molecules, whereas the enthalpy starts to decrease due to breaking of crystal structure, hence $G(\text{liquid}) < G(\text{solid})$. But in case of solid sample again the Gibbs free energy is distributed according to the stability of polymorph. For least stable polymorph, Gibbs free energy is much higher as compared to the most stable polymorph. This is because of their packing ability, so in case of SOS, the Gibbs free energy of all polymorphs changes as-

$$G(\alpha) > G(\gamma) > G(\beta') > G(\beta_1, \beta_2)$$

The transformation of polymorphs also takes place according to their stability. For example, in case of SOS, all polymorphs can form directly from molten liquid, however they can only transform sequentially like α to γ to β' to β_1, β_2 (i.e. inter-polymorphic transition is irreversible process). Due to such complexity in structure of TAGs (such as long carbon chain along with degrees of saturation), it crystallizes at lower temperature than that of its melting temperature.

Thus, such crystallization behavior of TAGs is important to study as fats and oils are used in almost all food products for various purposes and quality of final product is dependent on their physicochemical properties. Moreover, another factor to consider during crystallization of fats and oils is their rheological properties. The rate of inter-polymorphic transition between polymorphs is also dependent on the shear rate applied. Feuge et al., (1962) was the first to establish that in case of Cocoa Butter, the solid-solid transition between the polymorphs was accelerated by mechanical work during repetitive extrusion under pressure (\leq 1000 psi). Another research was on three fats- cocoa butter, milk fat and palm oil by Mazzanti et al., 2003. According to their study, shear encouraged the rate of phase transition from less stable to most stable polymorphic forms. Thus, nucleation and crystal growth of TAGs mainly depend on the cooling rate and shear rate applied during crystallization process.

In our study, Tristearin (TS), Cocoa Butter (CB) and Coconut Oil (CO) were considered for observing the changes in their thermal and physicochemical and rheological properties after mixing with each other.

Tristearin

TS is an easy model system as it is a monosaturated TAG composed of three stearic acid (SSS) with 18 number of carbon atom, and after crystallization it forms three polymorphs namely- α (less stable), β' (metastable), β (highly stable) with melting temperatures of 54°C, 65°C and 72.5°C respectively (Windbergs, 2009). It has the characteristics of crystallizing suddenly whenever it reaches the temperature below its melting point, similar to candle wax; therefore it is usually used as a hardening agent in candle and soap production. Another interesting fact is that as it is monoacid triglyceride, it forms perfect crystalline structure after crystallization process and also it is usually present in CB but in very small amount (Loisel et al., 1998) and therefore it was interesting to observe the possible changes that would occur after blending of TS and CB.

Cocoa Butter

Cocoa Butter (CB) is a fat manufactured from the cocoa beans during roasting process. These cocoa beans are taken out from cocoa tree (*Theobroma cacao L.*), which is also called 'chocolate tree'. The cocoa tree originates from South and Central America, but now it is grown commercially at most of the places in the world where the temperature is above 27 °C and there is a constant high humidity throughout the year (Beckett S. T., 2000). Hence, the composition of CB differs according to the region of cultivation, climate conditions, etc., and due to such differences in TAG composition, it is a difficult task for industrial personnel to form good food product quality for each time. Therefore, it is necessary to study the

crystallization of CB more thoroughly since its main application is in the chocolate production and their confectionaries. About 1/3rd of chocolate is made up of CB additionally it also helps to maintain good quality of chocolate (Sonwai et al., 2006). The composition of CB consists of monounsaturated symmetrical TAGs, which are POP (1,3-dipalmitoyl-2-oleoylglycerol), POS (1,3-palmitoyl-stearoyl-2-oleoylglycerol) and SOS (1,3-distearoyl-2-oleoylglycerol); where P-Palmitic Acid, O-Oleic Acid and S-Stearic acid (approximately 17% of POP, 37% of POS, 27% of SOS) (Loisel et al., 1998) and remaining composition consists of di-unsaturated and tri-unsaturated TAGs as well as, traces of polyphenols and free fatty acids. After crystallization of CB, six different polymorphs are formed and depending upon their stability, quality of chocolate is determined. In Table 1, the polymorphic forms and their melting temperatures are given (Wille et al., 1966). However, the melting temperature of these polymorphic forms differs according to the cooling process used for crystallization of CB. For instance, suppose Form I shows the melting temperature of 17.3 °C with cooling rate of 0.5 K/minute rate, if the rate changes the temperature would shift with small temperature difference.

Table 1: Different polymorphic forms of CB and their respective melting temperature

Polymorphic Forms	Melting Temperature (°C)
γ (Form I)	17.3
α (Form II)	23.3
β_2' (Form III)	25.5
β_1' (Form IV)	27.5
β_2 (Form V)	33.87
β_1 (Form VI)	36.3

In chocolate production, β forms are the most desired one because, it melts around human body temperature (~ 37 °C), which gives very good mouth feeling while eating chocolates. If the less stable polymorph is formed during chocolate production, then there would be a problem in stability of chocolate and eventually loss of quality.

Coconut Oil

Next model system considered was Coconut Oil (CO), which is extracted from kernel of mature coconuts. It consists of high amount of saturated fatty acids (~90%), with the

remainder being monounsaturated and polyunsaturated fatty acids. The TAG composition in CO is of various mixed saturated fatty acids, as- MLaLa, LaLaLa, MMLa, PMLa; where M- Myristic acid C(14:0), La- Lauric acid C(12:0), and P-Palmitic acid C(16:0), but mainly consists of lauric acid (~40%) (Danzl, 2015). After crystallization, these TAGs form polymorphs of α and β' crystalline structure and their melting temperature is very close to the melting temperature of CB (Jahrulu et al., 2014). CO can be used as a filling material in case of filled chocolate products and also in other confectionaries like in ice cream (chocolate coconut flavor ice cream), therefore it was another interesting example to study about its fundamentals of thermal properties when its mixed with CB and this will ultimately help to minimize the problems that occurred while preparing food products or during storage time.

The aim of this study was to determine the changes in fundamental parameters such as melting temperature, crystallization temperature, enthalpy change during heating and cooling process and changes in their crystal structure and morphology, also the changes in rheological properties after mixing Tristearin (which is a saturated fat) and Cocoa Butter (which consists of monounsaturated TAGs (Sat-U-Sat)) together. Additionally, we also studied the changes in thermal properties of another blend of Cocoa Butter and Coconut Oil (mixed short chained saturated TAGs).

Therefore the objective of thesis was divided into mainly four categories, which are as-

- 1) To monitor and compare the changes in melting and crystallization temperatures of different blends with individual fat/oil by using differential scanning calorimetry method.
- 2) To study change in crystal morphology and structural changes of blends with respect to individual lipids by using polarized light microscopy and X-ray diffraction respectively.
- 3) To observe the changes in rheological properties during the crystallization process by using parallel plate rheometer.
- 4) Effect of tempering on the crystallization process.

Chapter 2

Materials and Methods

2.1 Materials and general sample preparation

Cocoa Butter (CB), Tristearin (TS) and Coconut oil (CO) (Sigma-Aldrich GmbH, Germany) were used as a model system to study thermal and mechanical properties of individual fat/oil and in comparison with their respective blends. The blends were prepared in the ratio from 100% to 0% in steps of 10% for each experiment, as shown in Table 2.

Table 2: The ratio of amount of fat/oil in blends preparation

Blend 1		Blend 2	
Cocoa Butter (Weight %)	Tristearin (Weight %)	Cocoa Butter (Weight %)	Coconut Oil (Weight %)
100	0	100	0
90	10	90	10
80	20	80	20
70	30	70	30
60	40	60	40
50	50	50	50
40	60	40	60
30	70	30	70
20	80	20	80
10	90	10	90
0	100	0	100

General sample preparation:

- 1) Water bath (IKA, RCT) was heated at 70°C with the stirring speed of 450 rpm.
- 2) For each blend firstly CB was heated for 2 minutes until it was completely melted and afterwards the next fat or oil was added in the respective ratio.
- 3) This mixture was then heated further for 5 minutes so that the remaining fat/oil melts completely and during this the sample was stirred continuously with the help of glass rod.

Each sample was then analyzed using different techniques mentioned below. There were five techniques used for studying the thermal and physicochemical properties of above mentioned blends and those are as follows.

2.2 Techniques used to carry out the experiments

A) Differential Scanning Calorimetry (DSC)

DSC is a thermo-analytical technique, which was used to detect the phase change behavior i.e. changes in melting and crystallization temperature of fats and oil after mixing with each other.

i. Working Principle of DSC

This technique works on the principle of difference in the heat flow between reference crucible and sample crucible as a function of temperature and time. In Figure 7, the general setup for DSC is shown. It consists of an oven which has an empty aluminum pan as reference crucible and a sample crucible with certain amount of material in it. When melting and/or crystallization process occurs, the phase transition heat is measured in the sample with respect to the empty crucible and which is then recorded as a peak (Figure 8). The peak area corresponds to the enthalpy change (ΔH) during the process and its direction designates whether the process is endothermic or exothermic.

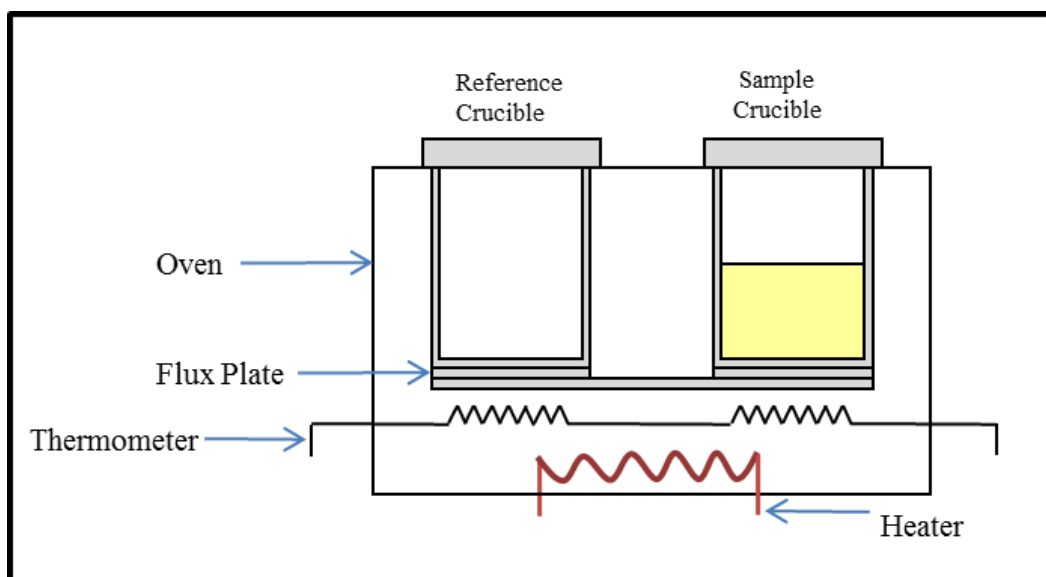


Figure 6: Working Principle of DSC including the general setup (modified from Beccard S.).

The difference in heat flow is described by the formula given below.

$$\Phi_S - \Phi_R \sim \Delta T$$

Where,

Φ_S – heat flow required for sample (W/g)

Φ_R – heat flow required for reference (W/g)

ΔT – Change in temperature ($^{\circ}\text{C}$)

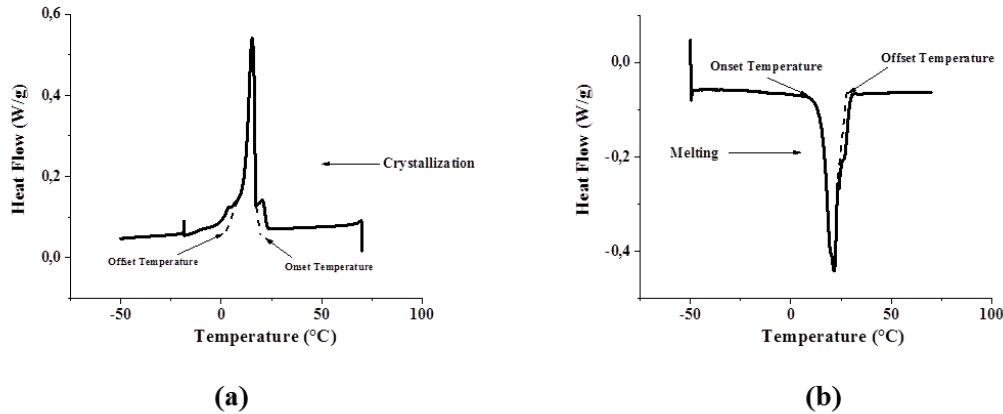


Figure 7: DSC thermograms for phase change behavior; (a) for crystallization process (exothermic); (b) for melting process (endothermic).

In Figure 8, the graphical representation of normalized heat flow with respect to temperature for crystallization and melting process are shown. In case of crystallization process, heat is released due to exothermic process, whereas, the heat is to be taken in the system to carry out the melting process (endothermic process), which is certainly recorded as a peak. The onset and offset temperature represents the start and end of process (crystallization or melting) respectively along with peak temperature as the crystallization or melting temperature of the system.

ii. Sample Preparation and experimental parameters

The blends were prepared as explained in section 2.1 and kept at room temperature overnight in a 2 mL eppendorf tube and then the DSC (Mettler Toledo DSC3+/700/453) measurements were carried out. Liquid nitrogen was used for cooling with the rate of 30 mL/minute. For sample preparation about 10 to 20 mg of blend was weighed in a 100 μL of Aluminum crucible and sealed it with Aluminum lid, and 100 μL of empty Aluminum pan was taken as a reference cell. Then the whole experiment was performed in three segments in order to observe the effect of cooling process on the crystallization of fat/oil and their respective blends. In Table 3 the detail description for these segments is given. As fat/oil sample was prepared one day before DSC measurement, the crystallization was occurred in different

manner than with 2 K/minute of cooling rate (in segment 2). Therefore, three segments were selected for measurement. The evaluation of the graphs was carried out in STARe software.

Table 3: Three segments for measurement in DSC

Process	Temperature Range (°C)	Heating/Cooling rate (K/minute)
Melting Process	20°C to 70°C	2
Crystallization Process	70°C to -50°C	2
Re-melting Process	-50°C to 70°C	2

B) X-Ray Diffraction (XRD)

XRD technique was used to determine the long and short-spacings in the crystal lattice, in order to define the crystalline structure. Long-spacings in lipid system represents the length of stacking of TAG molecules, which could be described as chain length structure (2L or 3L), whereas, short-spacing in each polymorphic form associated with the sub cell of the structure arise from the unit cell formed from TAG packing. TAGs crystallizes basically in three kinds of polymorphs as α , β' , β with respect to their increase in stability. The typical schematic of sub cell chain packing of these polymorphs is shown below.

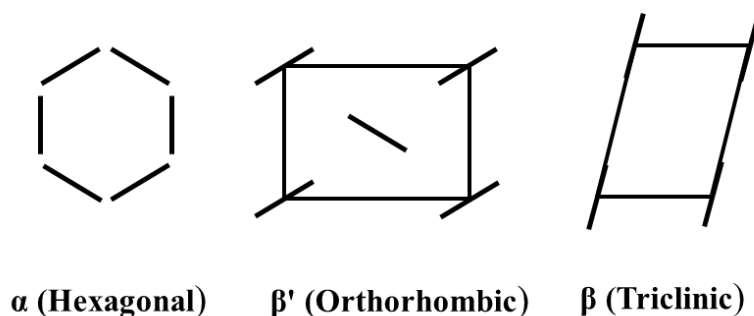


Figure 8: Schematic representation of sub cell chain packing structure which is commonly found in TAG polymorphic forms (top view of crystal planes) (Modified from Sato K., 1999).

i. Working Principle of XRD

This is an analytical technique used for determining the crystal structure of the material. It works according to the Bragg's law. In Figure 10, the basic principle for Bragg's law is given. The X-Ray beam from the source with a certain wavelength (λ) incident on the crystal lattice,

then the beam scatters with an angle Θ . The co-relation between scattering angle and X-ray beam wavelength is shown in equation 1, which is called as Bragg's law equation.

$$n\lambda = 2d\sin\Theta \dots (1)$$

d- Interplanar spacing

λ - Wavelength of x-ray beam

Θ - Scattering angle

By rearranging equation 1, the long and short-spacing are calculated.

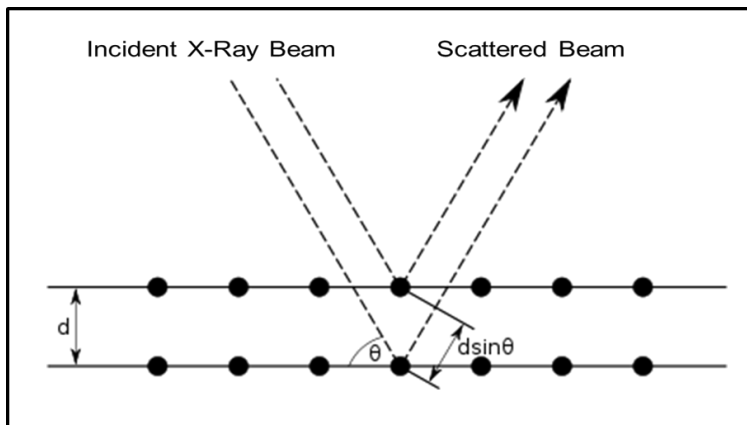


Figure 9: Schematic diagram representing Bragg's law principle.

In Figure 11(a), the general setup for experiment is shown. The X-Ray generator creates the X-ray beam. The X-rays are produced by an electron bombardment of a water cooled anode. Copper is often used as a target and after bombardment the electrons get excited, hence the kinetic energy transformed into photon energy. After reaching to higher energy level the electrons comes to its original position and that's when radiation ($\text{CuK}\alpha$) is emitted. This X-ray beam was then incident on the sample with a wavelength ($\lambda = 0.1542 \text{ nm}$, Copper as target) and afterwards it diffracted with an angle of 2Θ (Wim H., 2016). This diffracted beam was detected by a 2D detector, which is shown in Figure 11. Afterwards, the diffractogram was plotted between intensity and 2Θ by using Datasqueeze software (Figure 11 (b)). Based on diffracted angle, the long and short-spacings are to be calculated. The angle between 0 to 5° is to be associated with long-spacing and above 5° angle for illustration of the short-spacing in the crystal structure.

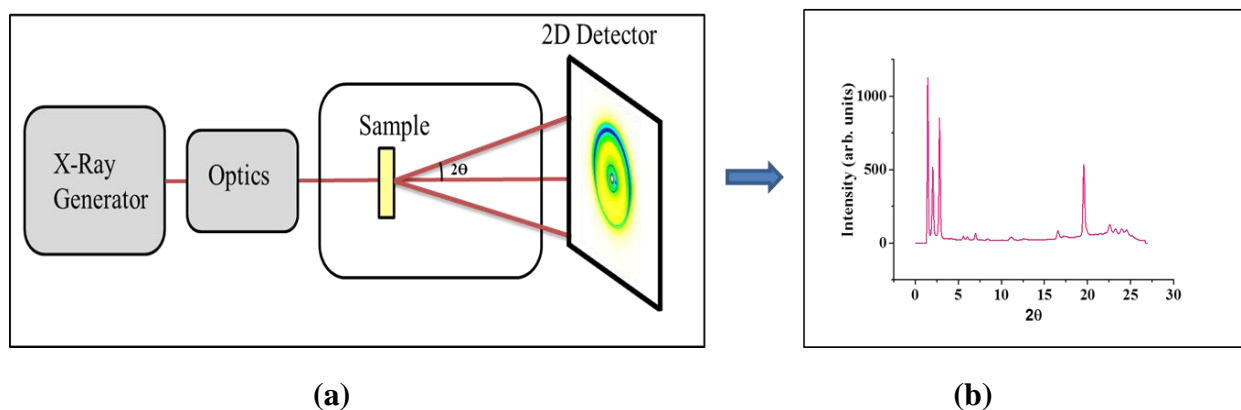


Figure 10: (a) Experimental setup of XRD; (b) Diffractogram (Modified from Gits Magazine).

ii. Sample preparation and experimental parameters for XRD

The preparation of blend was done as shown in section 2.1 and it was stored in marktubes (Image1) (Hilgenberg GmbH, Germany) with the following specifications.



Length – 80 mm, thickness- 0.01 mm and outer diameter – 1.50 mm

Image 1: Marktubes used as a sample holder to carry out measurements in XRD.

For pouring the sample in the marktubes, the needles and syringes were used. As, TS has tendency to become solid if it gets in contact with material having less temperature than its melting point, therefore needles and syringes were preheated by using the vacuum oven (Heraeus; ThermoScientific) for 5-10 minutes. These samples were then stored at room temperature for 22 ± 2 hours and afterwards analyzed in XRD. Aluminium Oxide (Al_2O_3) was used for calibration of scattering angle with respect to the sample to detector distance. Afterwards, the marktube containing sample was placed in the sample holder and arranged such that the part of a marktube used as a target for X-ray beam should be exactly in centre for getting the proper measurement. The whole experiment was performed for 30 minutes in the range of 0 to 30° of 2θ with time speed of 1 minute per degree.

C) Polarized Light Microscopy (PLM)

Microscopy was used to observe the changes in crystal morphology of CB and TS after mixing them together.

i. Working principle of PLM

The state of polarization of light source is changed when it is reflected or transmitted through a material which has optical property called birefringence. This physical property of a material represents the specific refractive index that ultimately defines the way of polarization and propagation of a light beam (Figure 12(a)) (Oldenbourg, 2013). PLM consists of one polarizer, one analyzer, condenser lens, tube lens, objective and sample platform. Polarizer is situated below the sample whereas; analyzer is placed above the objectives.

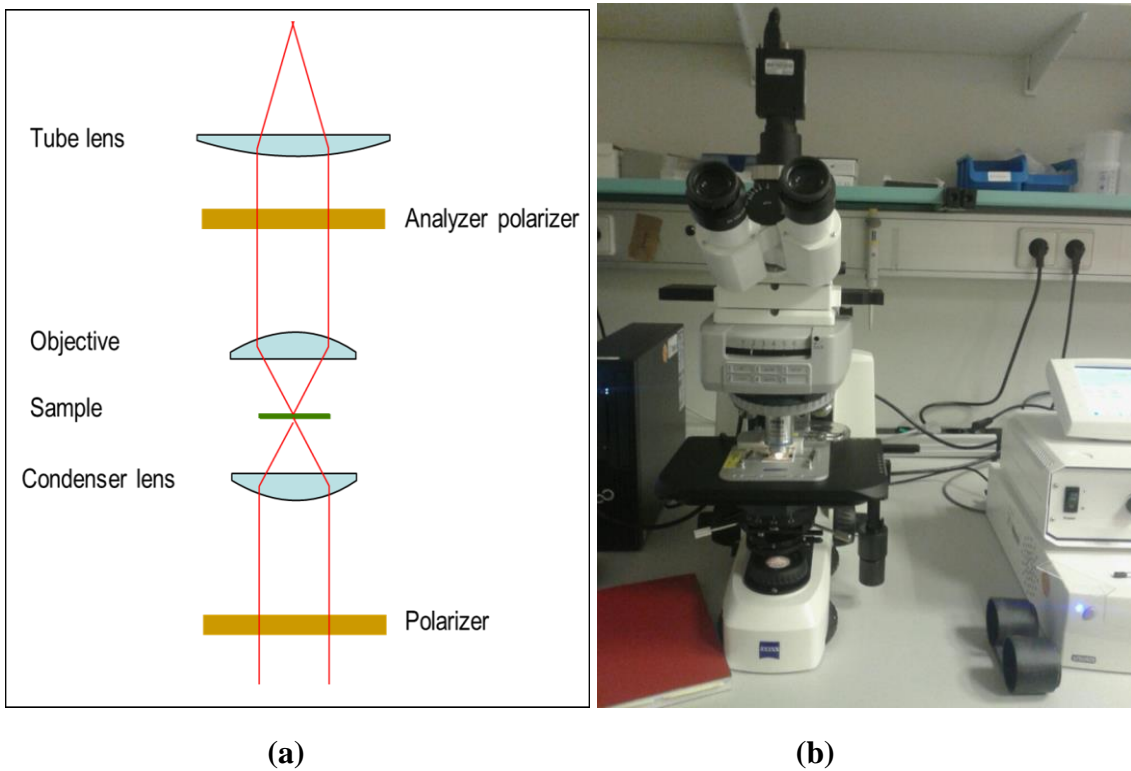


Figure 11: (a) Principle of PLM; (b) Experimental Setup for PLM

When light source from below, which is illuminating in all direction incident on the polarizing filter, it starts to follow one pathway in one direction. This propagation of light is either in circular form or in elliptical form. In our study the crossed polarization was used with the $\lambda/4$ plate (circular polarized light) in between polarizer and analyser. Afterwards, this polarized light incident on birefringent specimen, and it transmitted and passes through the analyzer which is in 90° to polarizer. Eventually the crystalline regions of specimen appear

bright which can be seen either through eyepiece or through camera shown in Figure 12(b) (Zeiss Scope. A1 Pol).

ii. Sample Preparation and experimental parameters

The same sample preparation method was used as analogous to DSC experiment. For measurement, firstly the sample was placed on microscope slide in powder form, which was then covered with cover slip. The peltier plate (Linkam, model PE120) was used to heat and cool the sample. The whole experiment was performed in three segments, which is similar to the DSC experiment. In Table 4, the segments are given specifically.

Table 4: Three segments for measurement in PLM

Process	Temperature Range (°C)	Heating/Cooling rate (K/minute)	Soak Time (Minutes)
Melting Process	22°C to 70°C	2	5
Crystallization Process	70°C to 10°C	2	5
Re-melting Process	10°C to 70°C	2	-

The soak time was provided for complete melting and crystallization of the samples.

D) Parallel Plate Rheometer

Parallel plate rheometer was considered to determine the crystallization behaviour under shear condition. CB and TS blends were considered for observing the changes in the crystallization starting temperature and its comparison with the DSC results.

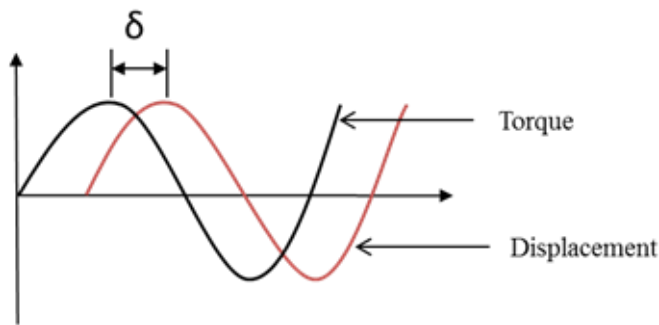
i. Working Principle

The experiments were performed by using the principle of oscillatory shear rheometry. When torque (stress) is applied to sample at an angular frequency (ω), then the change in displacement (strain) occurs. Hence, how much change in displacement has occurred due to the applied stress ultimately gives the viscosity and viscoelastic property of the material and this response is observed in terms of sinusoidal waveform (Figure 13). Below is the equation given for oscillatory shear rheometry.

$$\gamma = \gamma_0 \sin \omega t$$

$$\sigma = \gamma_0 (G'(\omega)\sin \omega t + G''(\omega)\cos \omega t)$$

$$\tan (\delta) = G''/G'$$



Where,

γ = strain, ω = angular frequency,

σ = stress, G' = storage modulus,

G'' = loss modulus, δ = phase angle.

Figure 12: Sinusoidal waveforms for torque and displacement.

Phase angle distribution represents the type of material characteristic, i.e. $\delta=0^\circ$ represents the purely elastic material (ideal solid) and if $\delta=90^\circ$, it behaves as a purely viscous material (ideal liquid). The condition where, δ is in between 0 to 90° i.e. $0 < \delta < 90^\circ$, the material shows the viscoelastic characteristic and at 45° , it represents the boundary of solid like and liquid like behaviour (which means start of nucleation process in case of lipid systems). After measurement of sample, the results can be obtained in terms of storage modulus (G') - modulus of elasticity i.e. storage of energy; loss modulus (G'') - viscous modulus i.e. energy dissipated as heat; and measure of damping ($\tan(\delta)$), which is the ratio of loss modulus to storage modulus. The graphical representation is shown in Figure 14(b). In Figure 14(a), the general setup for parallel plate is shown. In which the lower plate is fixed and the peltier heating/cooling system is attached to it, whereas the upper plate is moving with an angular frequency (ω).

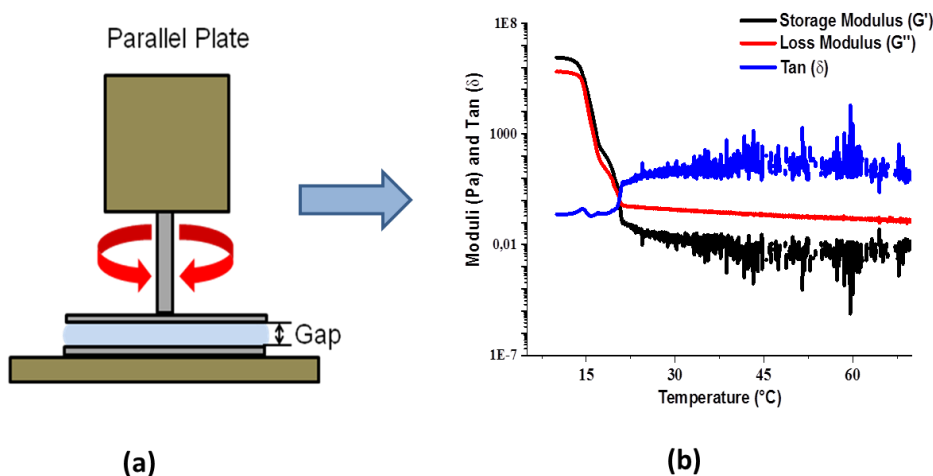


Figure 13: (a) General experimental setup for parallel plate rheometry; (b) Graphical representation of measured data of sample.

ii. Sample Preparation and parameters used for experiment

The parallel plate rheometer (Hybrid Discovery HR-3) was used to perform the experiment, which is shown in Image 2(a). To measure the viscoelastic properties in the rheometer, 40 mm diameter plate was used. Before starting the measurement of sample, the calibration was done for 40 mm geometry within the temperature range of 70 °C to 10 °C by using TA instruments software to determine the thermal expansion of the plates due to heating. Afterwards, the temperature of rheometer set to 70 °C and the two plates were kept close to each other to ensure homogeneous temperature in the sample and which was then covered with the thermal insulator as shown in Image 2(b). In the meantime, the blend was prepared as given in the section 2.1 and before the sample was poured on the lower plate, the gap was again zeroed. In case of lipid systems, with one set of parameter, it was hard to measure correct values as it transformed from completely liquid to solid form. The parameters used for experiment are shown in Table 5. For measurements axial force control (0 N) has been employed to ensure proper contact when the sample is shrinking due to change in volume during crystallization process. Also, maximum limit for torque was set to 30000 $\mu\text{N}\cdot\text{m}$ to avoid the damage to the instrument in case of higher torque value. The evaluation of graphs was performed in origin software.

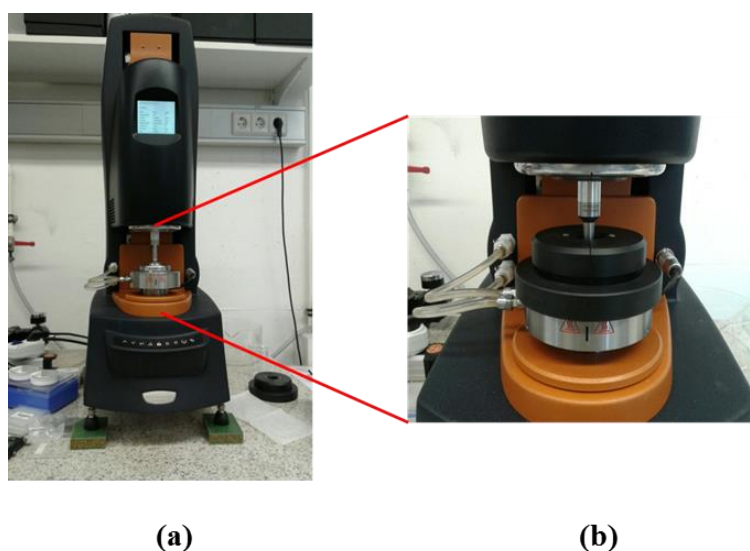


Image 2: (a) HR-3 Rheometer; (b) Thermal insulator for controlling the temperature gradient.

Table 5: Experimental parameters for rheology

Parameters used for experiment	Values
Start Temperature	70°C
End Temperature	10°C
Soak time at 70°C	5 minutes
Cooling ramp	0,5 K/minute
Strain (%)	0,001
Axial Force	0 N
Frequency	1 Hz
Torque	30000 μ N.m
Gap	500

E) Tempering process

The purpose of tempering process is to form the nuclei of thermodynamically stable polymorph which leads to formation of crystals with higher stability after complete crystallization of fat/oil. It can be done with or without shearing of the fats and oils at controlled temperature (Quinones-Munoz, et al., 2010). This temperature should be considered below the melting temperature of stable polymorph. For instance, generally in all lipid system, β is the most stable polymorph and the melting temperature differs according to the composition of TAGs but to attain the nuclei of this polymorph during crystallization process, the temperature to be selected slightly below its melting temperature. In case of CB and TS, the tempering process was carried out by using two methods, which are as follows.

i. By using closed water bath

Pure Cocoa Butter and Tristearin were melted individually in a beaker at 70 °C by using water bath and then placed in an Eppendorf tube, which was then sealed in a vacuum bag. Simultaneously, two closed water bath were set to 27 °C and 60 °C for Cocoa Butter and Tristearin respectively, as the β_2 (Form V) polymorph of CB melts at 33 °C and β' of TS melts at 62 °C. Afterwards, the sample was kept in a closed water bath for 20 hours and then the effect of tempering was examined by using DSC experiment. The disadvantage of this method

is that the low temperature is difficult to maintain for longer time. So to avoid such situation the constant climate chamber was decided to use for further measurement.

ii. By using Climate Chamber

For performing the tempering process, the KMF 115 (BINDER GmbH, Germany) constant climate chamber was used. The heating/cooling rate inside the chamber is of 1.5 °C/minute and relative humidity parameter was not taken into account during tempering process. The procedure used for tempering is given in Table 6.

Table 6: Steps used for tempering process in climate chamber

Sample Name	Temperature (°C)	Duration (hours)	Shear (stirring)	Purpose
Cocoa Butter (CB_tempered_#1)	60	15	No	Complete Melting
	30	2	No	Cooling without seed Formation
	27	1	No	Cooling with homogeneous seed formation
	32	2	No	Melting of unstable polymorph
Tristearin	60	15	No	Same conditions were selected so that comparison can be made with Cocoa Butter
	30	2	No	
	27	1	No	
	32	2	No	
Cocoa Butter	60	15	By using Magnetic Stirrer with the speed of 350 rpm	Complete Melting
	30	2		Cooling without seed Formation
	27	1		Cooling with homogeneous seed formation
	32	2		Melting of unstable polymorph

The temperature range was selected as mentioned in Industrial Chocolate Manufacture and Use, and time and stirring values were selected by trial and error method. The effect of tempering was then measured in DSC after storing the sample at room temperature for 7.30 hours as the CB was in liquid form after taking out from climate chamber.

Chapter 3

Results and Discussion

3.1 Analysis of thermal properties for different blends using DSC

By using Differential Scanning Calorimetry (DSC) technique, the changes in thermal properties (melting, crystallization and (ΔH) change in enthalpy during phase transition) of individual fat or oil (CB, TS and CO) with respect to their mixtures (CB+TS and CB+CO) are observed. This whole experiment was performed in three segments (explained in Table 3) to study the effect of cooling process on the polymorphic formation.

3.1.1 Blends of Cocoa Butter (CB) and Tristearin (TS)

In our study the blends of CB and TS were considered because, TS consists of pure saturated fatty acid and CB is a mixture of monounsaturated fatty acid containing TAGs along with various other components (described in introduction). Therefore, it was interesting to observe the changes in thermal properties after mixing it together.

A) Segment 1: Melting Process

The DSC melting endotherm curves for the mixtures of CB and TS is shown in Figure 15. In which black curve represents the pure CB and purple colour curve represents the pure TS along with all other mixtures in between representing different colour codes respectively. In all thermograms, the peak temperature represents the melting temperature of the system and onset and offset point (fig 8 (b)) denotes the start and end of melting process. Each peak maxima is associated with the melting temperature of one polymorph, whereas shoulder peak could be attributed the presence of another polymorph. The first segment was performed from 20 °C to 70 °C with the heating rate of 2 K/minute The data obtained in this segment represented the melting of those crystals, which formed when the sample was allowed to cool at room temperature for overnight. The observations from the results of DSC measurements are as follows -

- a) In case of pure CB, two peaks were formed during melting process, which could be attributed to formation of two polymorphs, one at 30.7°C (main peak) and another at temperature 34.8°C (shoulder peak). Hence, according to study of Wille R et al.,1966, the polymorphic forms occurred in our result was Form IV (β_1') and Form V (β_2) respectively. Similarly in case of pure TS, one endotherm peak was at 48.3°C (really small peak) and another at 61.4°C (sharp peak) was observed. According to data

published in Windbergs et al., 2009, temperatures 48.3°C and 61.4°C represents α and β' polymorphic forms.

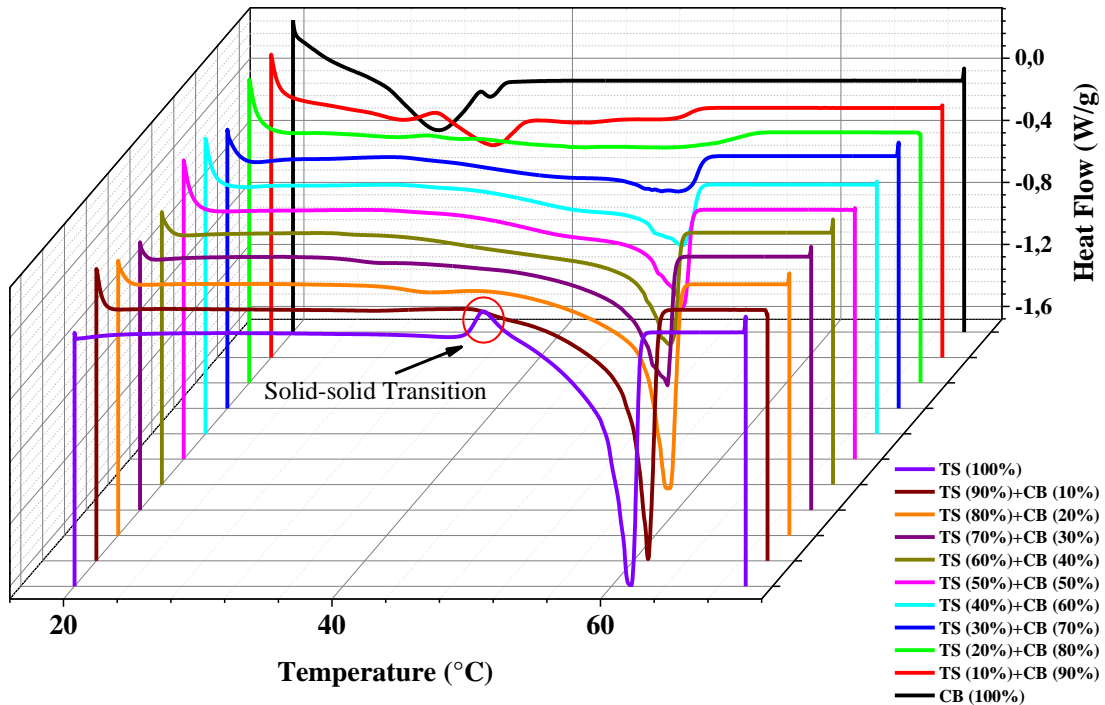


Figure 14: Melting endotherm of pure CB and TS along with their respective blends (CB-Cocoa Butter, TS-Tristearin).

b) After addition of CB in pure TS, the peak started to shift towards less temperature and the peak area also decreased accordingly. The change in melting temperature is shown in Figure 16 for each sample with respect to concentration of TS in each blend (as only one main peak is present in case of each blend). According to this result, the melting temperature decreased after addition of CB in TS. Such behaviour could be because of less molecular compatibility between CB and TS. The possible reason for less compatibility is the presence of double bond in CB (Sat-U-Sat TAGs), and after crystallization of these TAGs, the kinks (bend) are formed, whereas TS has ability to form perfect crystalline structure due to no double bond. So, when the interaction of these two kinds of different systems takes place, CB acted as an impurity for formation of perfect crystalline structure, which ultimately led to decrease in melting temperature.

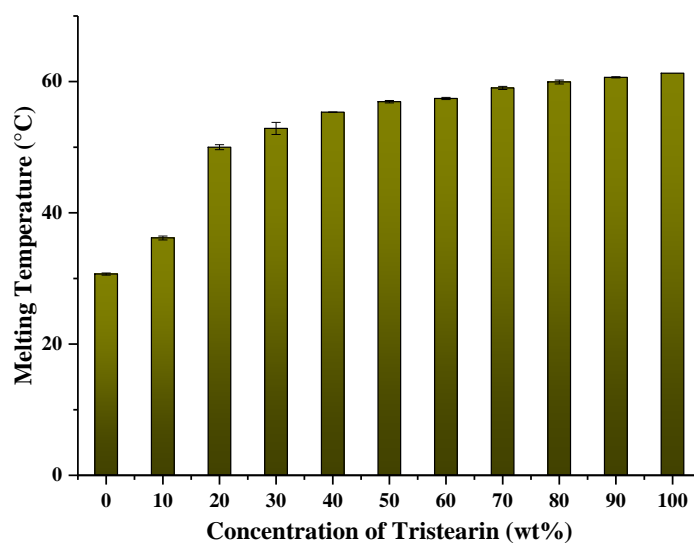


Figure 15: Evaluated data from DSC experiment showing the change in melting temperature (determined as a maximum of main peak) with respect to the concentration of TS in the mixture.

c) Another observation is, in pure TS curve, there was an exothermic peak observed during melting (shown in red circle, in Figure 17, for clear view plotted separately), this could be probably due to solid-solid transition in TS. This phenomenon occurred because of conversion of one polymorph to another during melting process. In case of pure TS, firstly α form was melted at 48.5 °C and then transformed into β' . But during transformation, the crystallization of β' occurred at temperature 50.51 °C and then it started to melt. According to Hagemman et al., 1988, the transformation from vertical α form to tilted β' could be due to collapse of hydrocarbon chains or from bending of each molecule in the glycerol region. However, still the specific reason for this transition is not clearly known. Another research with respect to polymorphic transition was shown in MacNaughtan et al., 2006, where they proposed that α form melted and was directly transformed into β form without formation of metastable polymorph, and similarly, β' transformed directly into β , where there was no sign of α . But in case of our results, α form was transformed into β' (according to temperature we observed above), this could be because of difference either in sample preparation or in rate of heating. On the other hand, after addition of CB, this exotherm peak was diminished, which could mean that only one polymorph was formed directly from molten liquid.

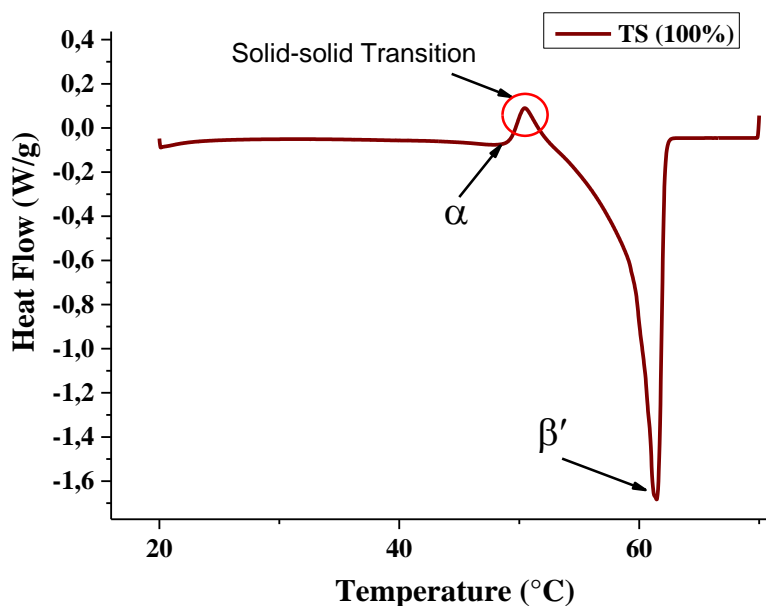


Figure 16: Representation of solid-solid transition in pure TS.

- d) After addition of 10% of TS in CB (TS (10%) + CB (90%)), the main peak was shifted towards more stable polymorph as compared to pure CB. It formed at temperature 36.67 °C (Form VI) which is the most stable form. But during measurement some traces of β_1' along with broad range of melting peak was also detected (Figure 18). This could imply that if only less percentage of TS is added in CB, it encourages the crystallization of CB, which is also verified by Davis and Dimick postulations. In their study of analysis of seed crystals, they found that, some minor component such as glycolipids (11.1%), phospholipids (6.6%) and saturated TAG (67.7%), promote the crystallization of CB.

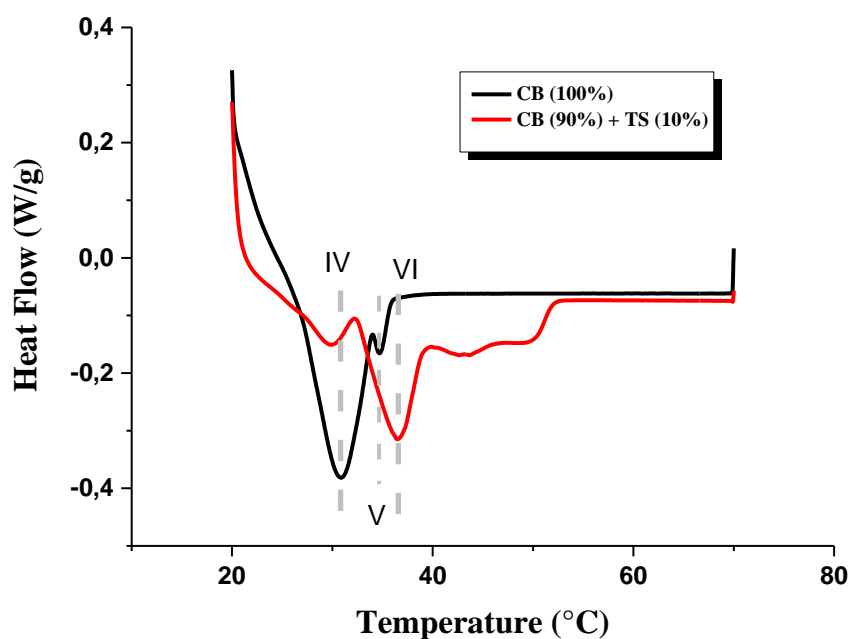


Figure 17: DSC recordings representing the change in polymorphic forms after addition of 10% TS in CB. Form VI was observed after addition of small amount of TS.

B) Segment 2: Crystallization Process

Next segment was to observe crystallization of molten liquid formed after melting process in segment 1 with the rate of 2 K/minute. The crystal memory was destroyed, after heating the sample at 70 °C in segment 1. This molten sample was then cooled to -50 °C with the rate of 2 K/minute. Controlled cooling process was achieved by this segment which led to formation different polymorphs from the cooling process achieved at room temperature before segment 1 and their polymorph formation can be studied during the cooling process in DSC. In Figure 19, the crystallization exotherm for all samples are shown. Again all colours represent a specific sample similar to segment 1. The observations achieved from Figure 19 are as follows-

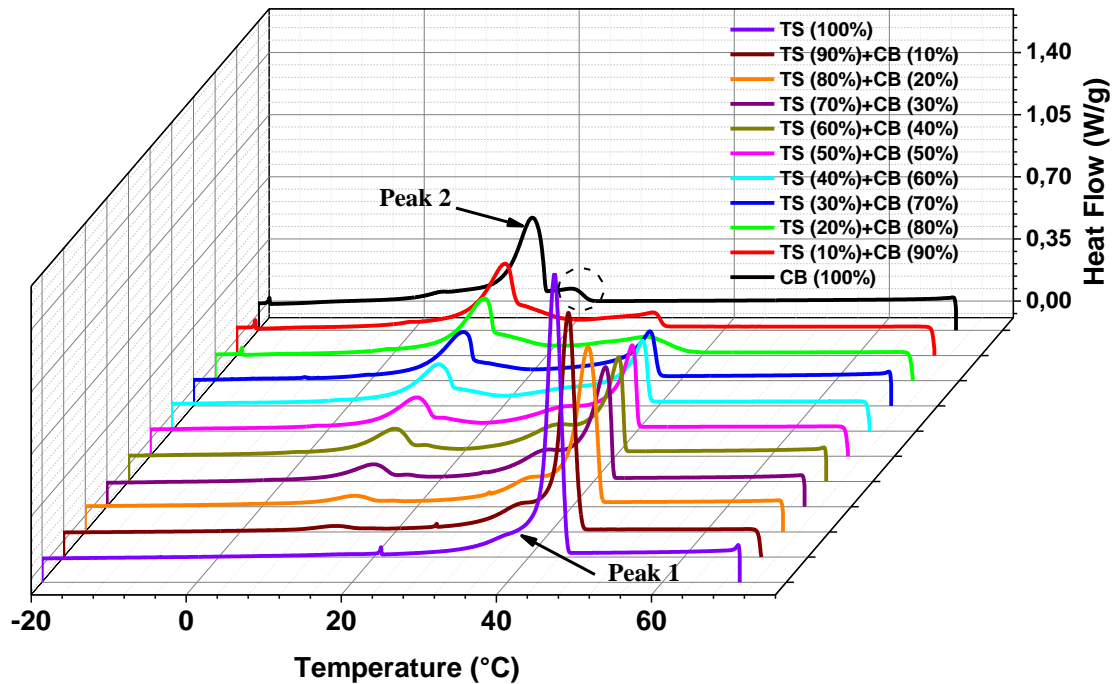


Figure 18: Crystallization exotherm detected by DSC (CB-Cocoa Butter, TS-Tristearin).

- a) From the peaks geometry, it was observed that there were 3 polymorphs formed in case of pure CB and 2 in case of TS. The stable polymorph crystallized at higher temperature as compared to less stable polymorph. Hence, in case of pure TS, the main peak attributed to the stable polymorph as compared to polymorph represented by shoulder peak. Whereas, in case of pure CB, one shoulder peak was detected before main peak, which implied that traces of more stable polymorph than that of the polymorph represented by main peak. However, in their respective blends, the shoulder peaks of both fats merged with each other, this could be because of the higher miscibility of these polymorphic forms with each other as compared to main polymorphic forms occurred.
- b) With comparison to pure fats, two exothermic peaks were detected in case of blends, in which peak 1 is for TS and peak 2 represents CB. As TS is a pure saturated fat, it crystallized at higher temperature than CB. Hence at 2 K/minute rate, TAGs of both fats could not get appropriate time for proper interaction with each other, which leads to inhomogeneous crystallization (therefore 2 peaks detected). Furthermore, Peak 1 shifted towards lower temperature after addition of CB in it and also the area of peak decreased accordingly. Whereas, in case of CB, only the peak area started to decrease

after addition of TS in it, there was not specific change in crystallization temperature of CB observed. The possible reason for such behavior could be the improper interaction between the structures of TAGs in CB and TS. Due to presence of oleic acid in CB structure, the chain packing becomes complex in nature. Therefore, TS could have encountered with difficulty in arranging themselves in closely packed manner. Whereas, in case of mixing two TAGs with at least one unsaturated fatty acid (in both of them), there could be less problems to pack themselves closer (Himawan C. et al., 2006). Hence in case of TS and CB blend, CB could be acted as impurity and this might lead to decrease in crystallization temperature (CT) of TS as concentration of CB increased in it (Figure 20(a)).

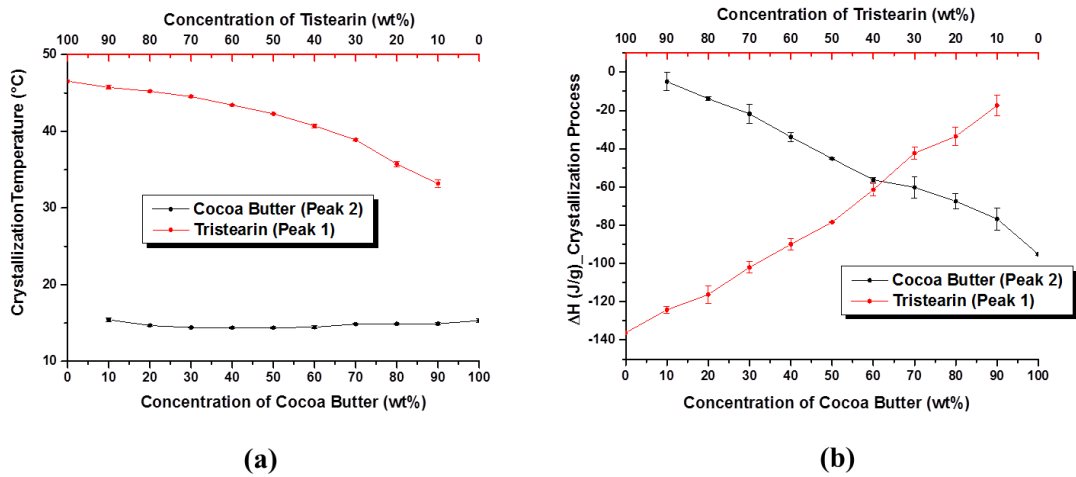


Figure 19: (a) Comparison of crystallization Temperature (CT) for CB and TS; (b) ΔH of crystallization vs. concentration of CB and TS.

DSC measurements were carried out in triplicates for statistical analysis and the evaluations of these peaks were carried out by using STARe software. As it was difficult to differentiate between the exact area for CB and TS in case of blends, the temperature limit was considered for calculation of integrated peak area. The area below temperature 23.13 °C was considered for CB and above it for TS in their respective blends. Analysed data from DSC thermogram is plotted in Figure 20(a) and (b). It is a graphical representation between crystallization temperatures and ΔH with respect to the concentration of CB (bottom x-axis) and TS (top x-axis) respectively (as crystallization is an exothermic process, the data (ΔH value) was considered with negative sign). The crystallization temperature for TS decreased after addition of CB in it, whereas, in case of addition of TS to CB, it was almost constant. This result of CB was in contrast with our expectation of changing the crystallization temperature

either in one of the direction. Since TS is a saturated fat which has a tendency to crystallize at higher temperature and this could act as a seed crystal in case of mixtures. Eventually, this might help to increase the stability of polymorphic forms of CB. However, according to the results obtained from this experiment, the ΔH for crystallization of polymorphs of CB decreased, which could mean that, the same polymorph was forming but with less stability due to loosely chain packing. Therefore, this was important question to find more in details as CB consists of combination of monounsaturated TAGs and after addition of TS (SSS), there was no effect on the crystallization temperature of CB. Whereas, ΔH required for the crystallization process was changing in both fats according to their concentration in the mixture.

C) Re-melting Process

Re-melting procedure was carried out for determining the melting temperature of polymorphs that occurred during crystallization process (segment 2) with heating rate of 2 K/minute. In Figure 21, the melting endotherms detected by DSC are shown. In which, similarly as segment 2, Peak 1 represents TS and Peak 2 represents CB. The observations made from these endotherms are as follows-

- a) In case of pure CB, DSC detected one sharp peak along with three shoulder peaks, which denotes that mixture (fusion) of four different polymorphs could be present in the system. In Figure 22, the graphical representation of 100% CB is shown, in which, 1, 2, 3 and 4 represents the four polymorphs accordingly and peak 2 represents the main peak. Based on their maximum peak temperature, it was established that γ , α , β_2' , β_1' polymorphic forms were formed respectively. Whereas, in case of first melting (segment 1), the melting temperature indicated formation of (Form IV) β_1' polymorph. This comparison clearly shows that polymorph formation in case of CB is dependent on the cooling rate.

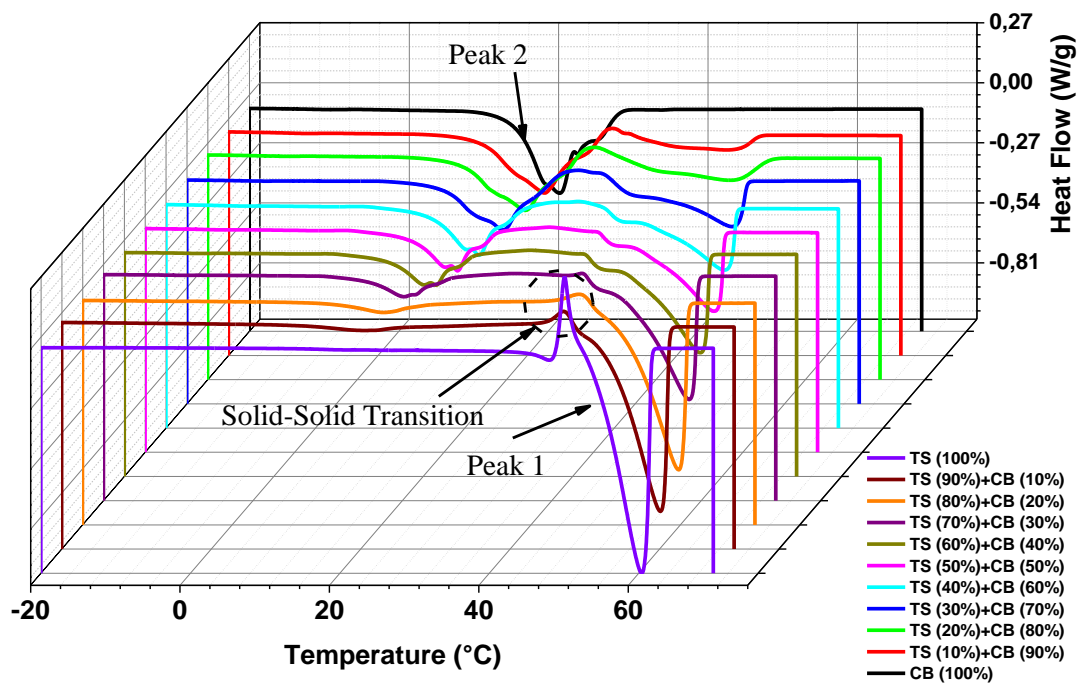


Figure 20: Re-melting Endotherm of pure CB and TS along with their blends (CB-Cocoa Butter, TS-Tristearin).

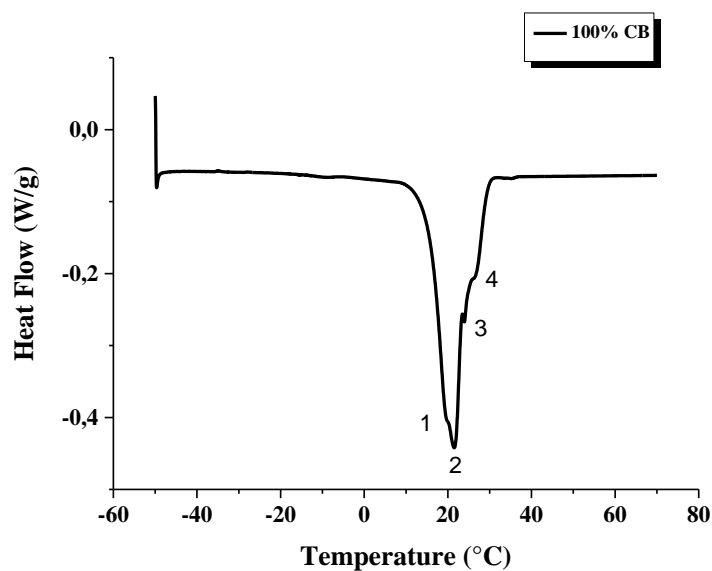


Figure 21: Melting segment of Cocoa Butter indicating the presence of different polymorphs in the mixture.

- b) In case of TS two polymorphs were formed (α , β'), which is similar in case of first melting (segment1). Only difference is that peak temperature of both polymorphs was slightly shifted from 48.5 °C to 48.0 °C and 61.2 °C to 60.2 °C respectively.
- c) Again, the melting temperature (MT) of TS decreased after addition of CB in it as similar to segment 1. However, the crystallization peak (solid-solid transition) did not vanish completely even after addition of CB. This indicates that under the controlled conditions of crystallization during segment 2, the presence of CB influenced the crystallization of TS less than that in case of crystallization at ambient conditions. The results of which had been probed in segment 1. As the cooling rate for crystallization process after sample preparation in water bath was quiet slow and TAGs in TS and CB had much more time for most favorable arrangement, this could have led to formation of one polymorph directly from liquid melt, however, in segment 2, the crystallization was faster and hence, less time was available for complete polymorphic transition (hence mixed crystal formation occurred).

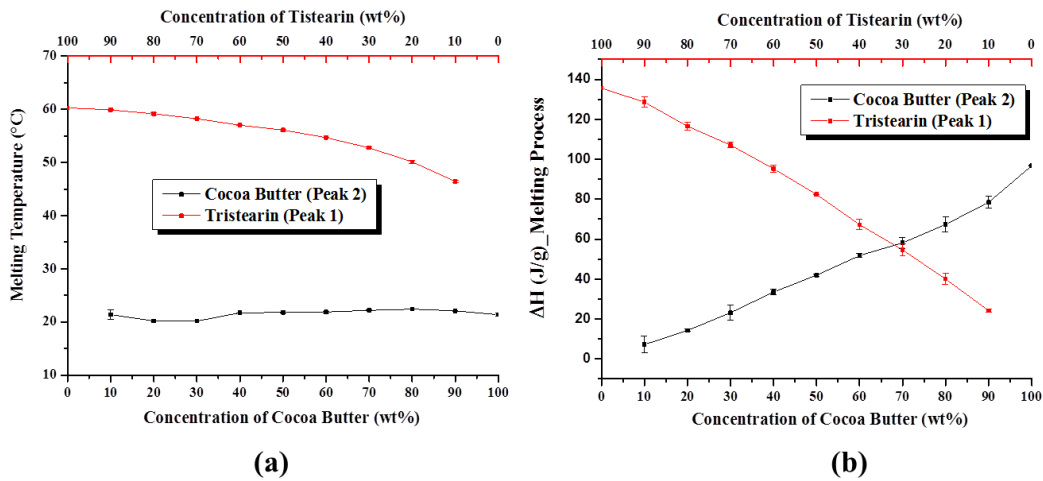


Figure 22: (a) Comparison of melting Temperature (MT) for CB and TS; (b) ΔH of fusion vs. concentration of CB and TS.

For evaluation of these endotherms again the temperature limit was selected, which was as-below temperature 31.06 °C, the area was considered as CB and above for TS. The data is plotted in terms of melting temperature and ΔH of fusion, in Figure 23 (a) and (b). Similar result was obtained in case of change in MT as of segment 2 (CT). ΔH (the enthalpy change required for melting of fats), was decreasing in both fats after mixing it together. Hence, ΔH of fusion (mixtures of crystals that were formed during crystallization) in case of pure CB was

$\sim 95 \text{ J.g}^{-1}$ and ΔH of pure TS was $\sim 136 \text{ J.g}^{-1}$. In case of CB, when TS was added, the ΔH value decreased simultaneously, which relates to the increase in Gibbs free energy (as the temperature was almost same). This speculated that the same polymorph could form but with less stability due to less dense crystal packing. Loisel et al., 1998, determined ΔH of fusion for each polymorph in case of CB. According to their study, the ΔH of fusion is increasing from Form II to Form VI respectively. The values are as shown in Table 7.

Table 7: Fusion enthalpies of TAG polymorphs in CB

Polymorphic Form	ΔH of fusion (J.g^{-1})
(α) II	86.15
(β_2') III	112.47
(β_1') IV	117.57
(β_2) V	136.73
(β_1) VI	148.02

From these values and our results together concluded that, individual polymorphic form required more enthalpy of fusion (during melting) as compared to the mixture of polymorphs. Therefore, in case of pure CB, the mixture of 4 polymorphs was formed with ΔH of fusion of $\sim 95 \text{ J.g}^{-1}$; this indicated that mixture of polymorphs is thermodynamically unstable as compared to the individual polymorph.

3.1.2 Blends of Cocoa Butter (CB) and Coconut Oil (CO)

After observing of changes in thermal properties of CB after mixing TS in it, Coconut oil was considered as a model system, to study the changes in thermal properties of CB. As CO consists of TAGs of short chained mixed saturated fatty acid, it was interesting to compare the changes in properties of CB in both blends. The experiment was performed as similar to CB/TS blend.

A) Segment 1: Melting Process

DSC detected the endotherm of mixtures of CB and CO and their comparison with the pure fat and oil is shown in Figure 24.

a) Generally, CO is in solid form at room temperature (in Germany $\sim 22^{\circ}\text{C}$), but it starts to melt immediately during handling. Hence, while preparing the sample for DSC measurement, the CO was in semi solid form and therefore during melting process, no sharp peak was detected. Similarly for most blends, there was no peak at all except in mixture containing 20%, 10% and 0% of CO in CB. So, from 30% CO onwards, the crystallization of CB was hindered so much that no crystals can be detected.

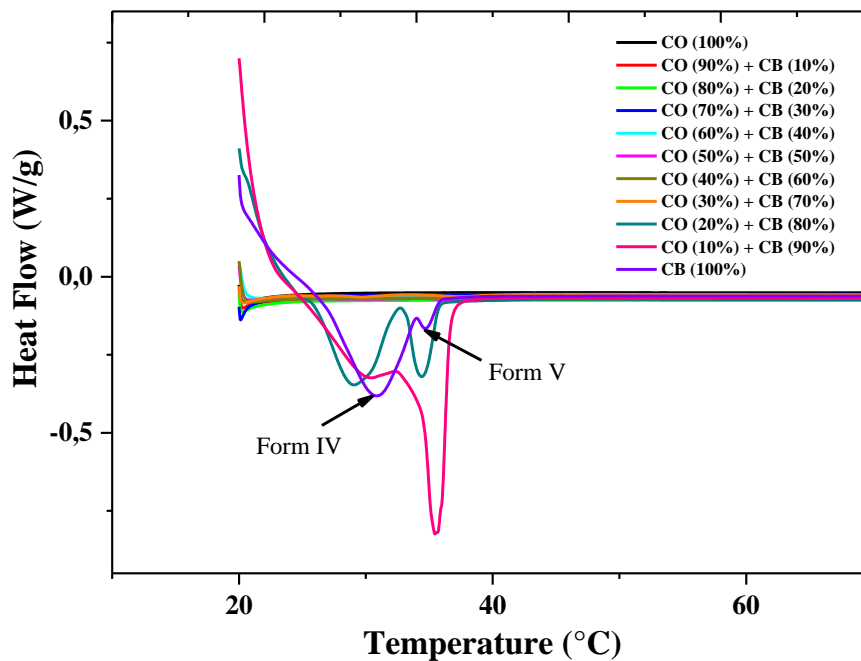


Figure 23: DSC endotherm for the mixtures of CB and CO.

b) The polymorphs formed in pure CB are as- Form IV represented by a sharp peak and Form V as a shoulder peak, similarly as explained in segment 1 from CB/TS blend. However, after addition of 10% CO, the same combination of polymorphs formed but in different ratio. In this blend (CO (10%) + CB (90%)); Form V become more prominent than it was in pure CB. On the other hand, if concentration of CO increased to 20%, then the polymorph ratio changed again. This could mean that only less amount of CO promotes the crystallization in CB (Figure 24).

B) Segment 2: Crystallization Process

In Figure 25, the exotherms are shown for CO and CB and their respective blends. In this thermogram, black curve represents pure CO and purple curve as a pure CB along with all mixtures in between. The observations obtained from this result are as follows-

- a) In case of pure CO, two crystallizations exotherm were detected, in which, one was sharp peak at lower temperature (2.5 °C) (Peak 1) and second peak overlaps in the same peak at higher temperature (7.4 °C) (Peak 1(a)). This could be because of incomplete crystallization of different TAGs in CO with 2 K/minute cooling rate. If the rate of cooling decreases, there will be possibility of complete crystallization of these short chained mixed saturated TAGs (CLaLa, LaLaLa, LaLaM, CCLa) as they could get sufficient time to arrange themselves properly (Tan et al., 2001).
- b) After addition of CB in CO, the different patterns were seen. At concentration of 10% CB in CO, just one peak was detected; this could be due to a shift of Peak 1 close to the position of Peak 1(a). However, after addition of 20% of CB, the peak again shifted back to lower temperature (green curve). In case of 30% of CB two peaks observed but it was difficult to interpret which peak represents CB, because after addition of 40% CB, three peaks are visible, of which the two at lower temperature probably results from CO crystals and the one at highest temperature from CB. The possible reason for such pattern could be the specific kind of interaction between TAGs in CO and CB which led to co-crystallization process. As the exact concentration of different TAGs in CO and CB were unknown in our case, the specific structure of different polymorphs in CB and TAGs of CO was difficult to determine only by DSC and hence it is hard to describe in detail how the interaction exactly take place.

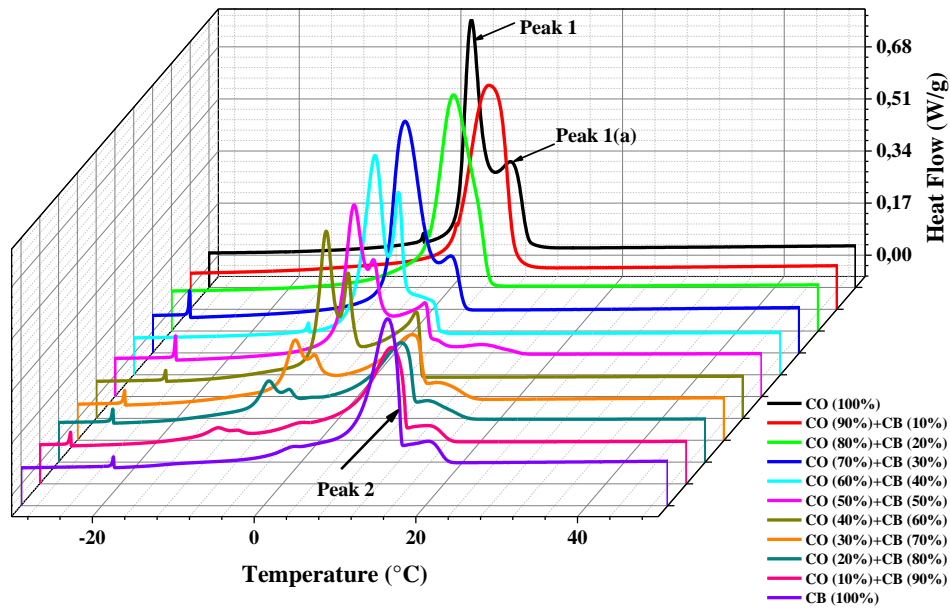


Figure 24: DSC exotherms for the mixture of CO and CB and their comparison with individual fat.

C) Segment 3: Melting Process

In Figure 26, the endotherms are shown for CB and CO and their blends (For clear view the heat flow parameter to be increased by the step of 0.2 W/g in each sample measurement). Similar colors represent the same samples as in crystallization process.

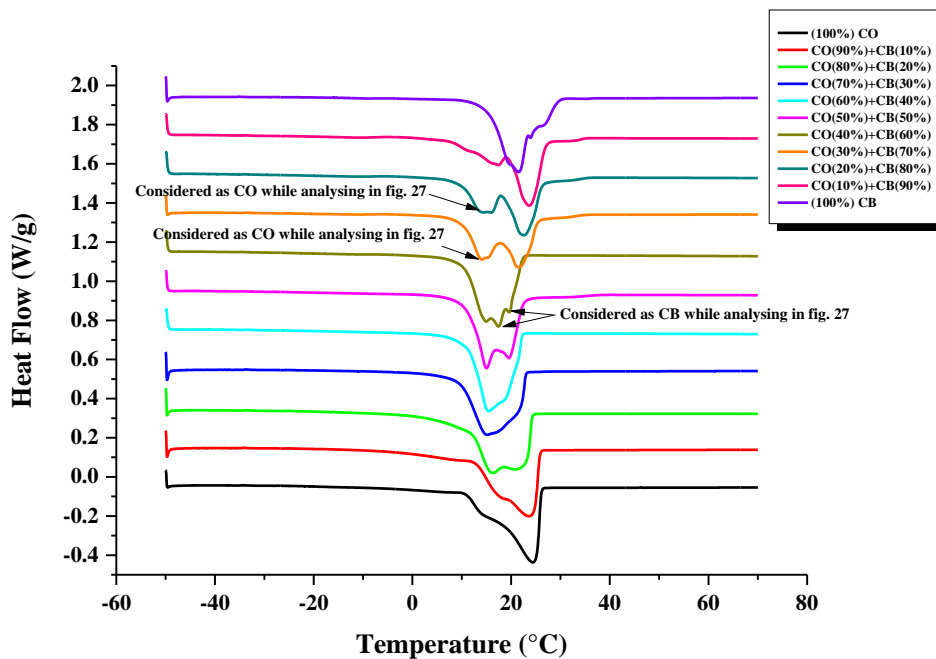


Figure 25: DSC endotherm for CO and CB and their respective blends in between.

The observations made from DSC endotherm are as follows-

- a) Pure CO melted with one peak at higher temperature (24°C) along with the shoulder peak at lower temperature (14.5°C). This could be similar to the crystallization process as two crystals were formed during cooling process. During melting process, more than one crystal from different TAGs melted simultaneously which led to the overlapping and eventually to the broad peak.
- b) After addition of CB in CO, the peak started to shift slightly towards lower temperature for 90% and 80% of CO and at concentration of 70% and 60% of CO (shown in blue and cyan color) only one endotherm was detected with slight presence of shoulder peak. This behavior is possibly explained as a eutectic mixture as there could be a formation of new molecular compound due to interaction between the short chained TAGs in CO and (Sat-U-Sat) TAGs in CB (Himawan et al., 2006). The properties of this molecular compound are yet to be revealed in near future.
- c) Another observation is as the concentration of CB increased further; the endothermic curves started to split into three different peaks, as two peaks could be from TAGs of CO and one with higher peak height and at higher temperature represents CB.
- d) In case of mixture of CO (10%) and CB (90%), the endothermic peak detected at higher temperature as compared to pure CB main peak. This behavior indicated that less amount of CO promotes the formation of stable polymorph in CB. The similar phenomenon was also observed in segment 1 melting process.

The evaluation of these endotherms was carried out by origin software and change in melting temperature with respect to concentration of CB (top x-axis) and CO (bottom x-axis) is plotted in Figure 27. In case of 60% of CB, evaluation of the endothermic peak was difficult to select the peak for CB in case of the mixture as it has three overlapped peaks. Hence both points considered and plotted differently in Figure 27 (shown in purple color). Also, in case of 30%, 20% and 10% of CO, the peak at lower temperature was considered between two peaks while plotting the graph; as at 50-50 wt%, two peaks were detected in which one which is at lower temperature to be considered as CO and so to consider the changes in temperature of only one crystal form, the lower temperature peak was chosen.

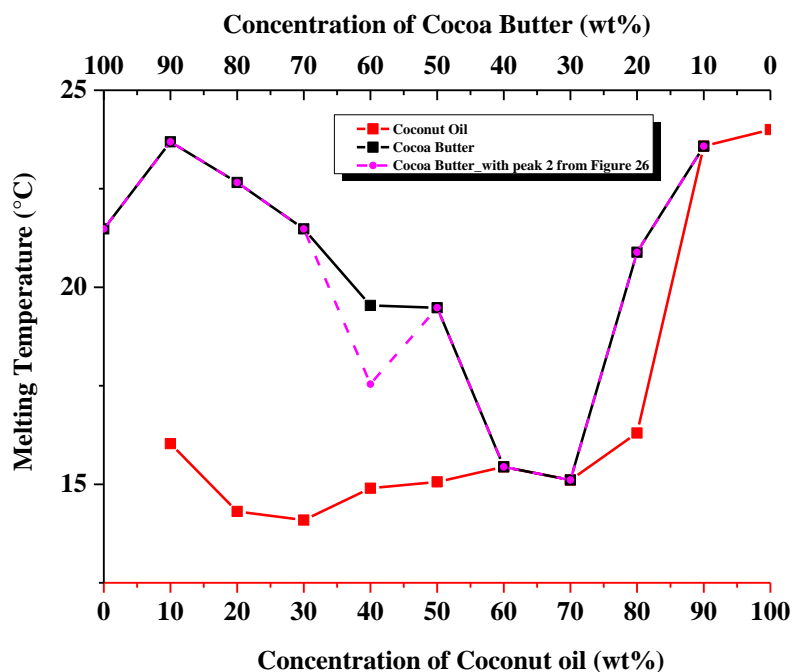


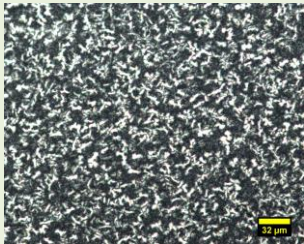
Figure 26: Data evaluation from DSC endotherm in terms of change in melting temperature of Coconut Oil and Cocoa Butter in their respective blends.

3.1.3 Comparison between blends of CB+TS and CB+CO

DSC results for blends of CB with TS and CO demonstrated that CB shows different characteristics after addition of fat/oil, depending on the TAG composition of the added component as it is shown in Table 8.

Table 8: Effect on CB after addition of TS (saturated fat) and CO (mixed saturated short chained TAGs).

Properties	Blend 1		Blend 2	
	Cocoa Butter	Tristearin	Cocoa Butter	Coconut Oil
Main TAGs	POP	SSS	POP	LaLaLa
	POS		POS	CCLa
	SOS		SOS	CLaLa
				LaMM

Polymorph occurrence	$\gamma, \alpha, \beta_1', \beta_2'$ β_1, β_2	α, β'	$\gamma, \alpha, \beta_1', \beta_2'$ β_1, β_2	No specific nomenclature for polymorphs, crystallization occurs due to interaction of saturated TAGs
Melting Temperature	Almost constant in blends	Decreasing after addition of CB	Decreased until 30% concentration of CB in mixtures and started to increase afterwards	Decreased until 30% concentration of CO in mixtures and started to increase afterwards
Mixture Occurrence	Non eutectic mixture		Eutectic mixture at concentration of 60 and 70% of CO in CB	
Molecular Compatibility	Low due to presence of oleic acid (kinks in the structure), hence hard to form closely packed arrangements		Also low compatible due to big difference in their carbon chain length. Only low amount of CO can be incorporated into CB.	
Crystal structure in PLM for 50:50 mixture	 <p>Needle like structure but not that sharp</p>		 <p>Microstructure formation due to CO</p>	

3.1.4 Phase diagrams for binary mixtures

For plotting phase diagram, weight fraction was considered instead of mole fraction as it was difficult to calculate the exact molecular weight of CB and CO because it contains mixtures of various TAGs.

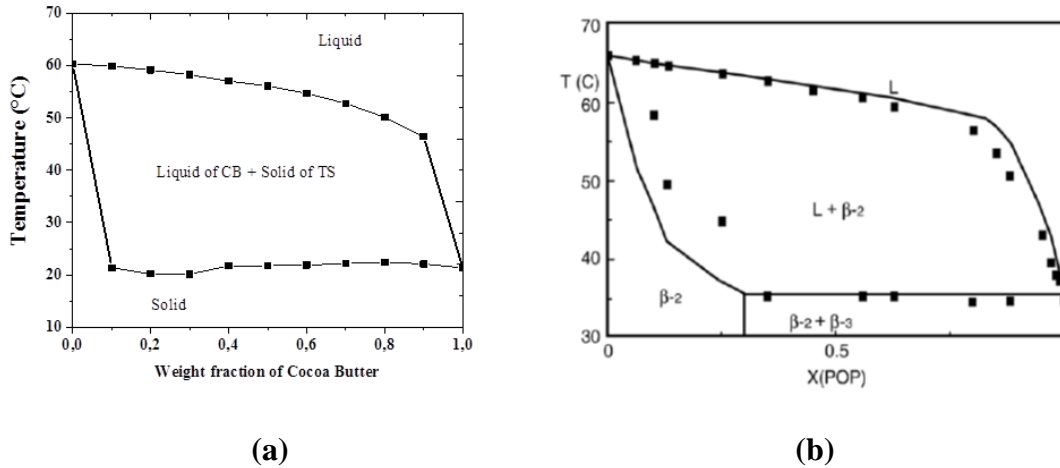


Figure 27: (a) Phase diagram constructed from calorimetry data of CB (POP/POS/SOS) and TS (SSS) blend; (b) Phase diagram for mixture of POP and PPP (Bruin, 1999).

In Figure 28(a), the phase diagram for CB and TS blends is shown. It consists of mixtures of crystal form α (CB) and β' (TS). The similar phase diagram was obtained in case of POP/PPP mixtures, which was studied by Bruin S, 1999 (Figure 28 (b)), in which data with black dots represent the experimental data and solid line represents the Margule's model fitted to data. The excess Gibbs energy for all solid phases was fitted using Margule's equation. For binary mixtures, the equation is as explained below.

$$\Delta G_E = (A_{21}x_1 + A_{12}x_2) x_1 x_2$$

$$RT \ln \gamma_1 = x_2^2 [A_{12} + 2(A_{21} - A_{12}) x_1]$$

$$RT \ln \gamma_2 = x_1^2 [A_{21} + 2(A_{12} - A_{21}) x_2]$$

In which, ΔG_E - The excess Gibbs free energy for solid phases, R- Universal gas constant, T-Temperature, γ_i - activity coefficient for one component in the mixture, x_1, x_2 - mole fraction of two components, A_{21} and A_{12} represents margule's parameters.

According to phase diagram (POP/PPP), formation of more stable polymorph in the mixture of both POP (β -3) and PPP (β -2) was obtained. This difference in crystal formation in both phase diagram (CB/TS and POP/PPP) could be because of two factors-1) the cooling/heating rate used in DSC could be different in both cases. 2) POP/PPP, systems are pure TAGs whereas, CB consists of various TAG composition. Hence it is hard to form one stable crystal structure. Another observation according to their study indicated that the interaction between monounsaturated (Sat-U-Sat) TAG and TAG of monosaturated fatty acid (PPP) could behave as monotectic partial solid solution (as the difference in melting temperature of TAG component is more). So in case of CB and TS, it also could be possible that, the mixture

behaves as a monotectic partial solid solution. However, in case of CB and CO, the eutectic mixture was obtained, (Figure 29). This could be because of the less difference in the melting temperature between them. In this phase diagram two parts of mixture of liquid of CO and solid of CB occurred and the stability of these polymorphs in these phases were differed with respect to the concentration of CO in the system.

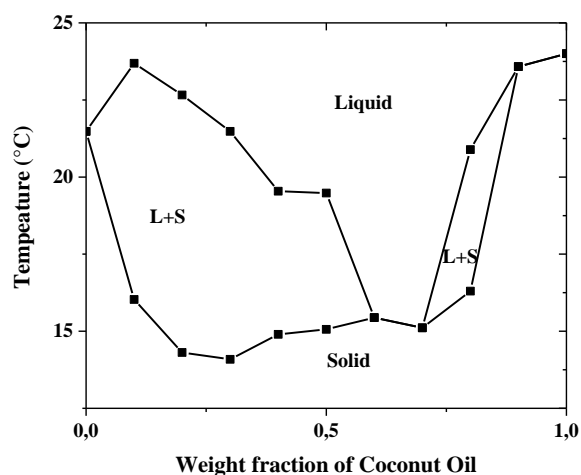


Figure 28: Phase diagram plotted from DSC data (considering melting temperature and weight fraction of coconut oil as a basis) of CB (POP/POS/SOS) and CO (LaLaLa/CLaLa/CCLa/LaMM) mixture.

3.2 Molecular structure analysis of CB and TS blends using XRD

As DSC is a thermo-analytical technique, which shows the changes in thermal properties, but to confirm which polymorph was exactly present and how the molecular structure of pure fat differed after mixing it with another fat was determined by using XRD method. In Figure 30, the results obtained from XRD experiment are shown. The different color represents different sample of blends along with pure CB and TS. Experiment was performed in duplicate for confirming the results. The long and short spacing detected over the range of 0 to 30° angle which is shown by arrow. These spacings were calculated by using Bragg's law principle.

$$n\lambda = 2d\sin\theta$$

For example, pure CB

$$n=1, \lambda = 1.54 \text{ \AA}, 2\theta = 1.99^\circ, 6^\circ, 20.51^\circ, 21.5^\circ$$

Then angle was converted to radian with the factor of 0.0174.

After putting these values in Bragg's law equation, the following values obtained (Table 9).

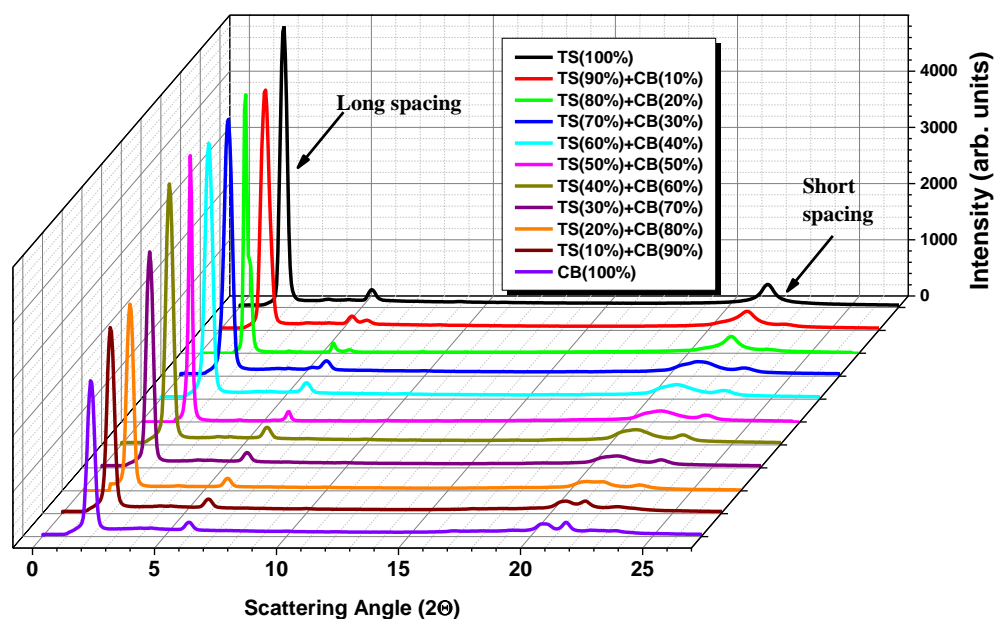


Figure 29: XRD reflexes for CB and TS and comparison with their blends.

Table 9: Comparison between the calculated spacings of CB and TS with literature values (vs-very strong; s-strong)

Sample	Angle (from experiment) 2θ ($^{\circ}$)	Calculated spacings from experimental data (\AA)	Literature given spacings (\AA)	Reference
Pure Cocoa Butter	1.99	44.47	45 (vs)	(Loisel et al.,1998)
	6	14.75	14.87 (s)	
	20.51	4.33	4.35 (vs)	
	21.5	4.14	4.15 (vs)	
Pure Tristearin	1.875	47.20	47	(Mayama, 2008)
	5.48	16.15		
	21.775	4.08		

After comparing these calculated spacings with literature known spacings, it is possible to say that in case of pure CB, Form IV (β_1') was obtained with the long spacing with chain length of $2L$ as it is mostly observed in case of POP triglyceride (Himawan et al., 2006). Also, in pure TS, only one spacing was found from literature (as shown in table 9) and after comparing it with the result obtained in our study, it could confirm that, the metastable polymorph (β') was

obtained. The similar observations were also achieved from the DSC results (segment 1). However, in case of blends of CB and TS, the observation from calculated spacing was not helpful to get into specific conclusion due to some errors during measurement. The possible errors were, while placing the sample in sample holder for measurement, there could be the error of adjusting center of x-ray beam exactly to the center of marktube, which gave some inaccuracy in measurement, and another problem was, there was a possibility of air bubble while pouring the sample inside the marktube. Therefore, there is still scope for optimization for correct measurement in case of blends. Another observation from Figure 30 was change in intensity of reflexes from pure TS to pure CB observed. After addition of CB in TS, the intensity of reflexes started to decrease as the concentration of CB increased. Whereas, in case of reflexes which detected at higher scattering angle (short-spacings representing peaks), become broader in mixtures of 30% to 70% of CB. Therefore, it is important to study how the interaction of different mixture of polymorph occurred.

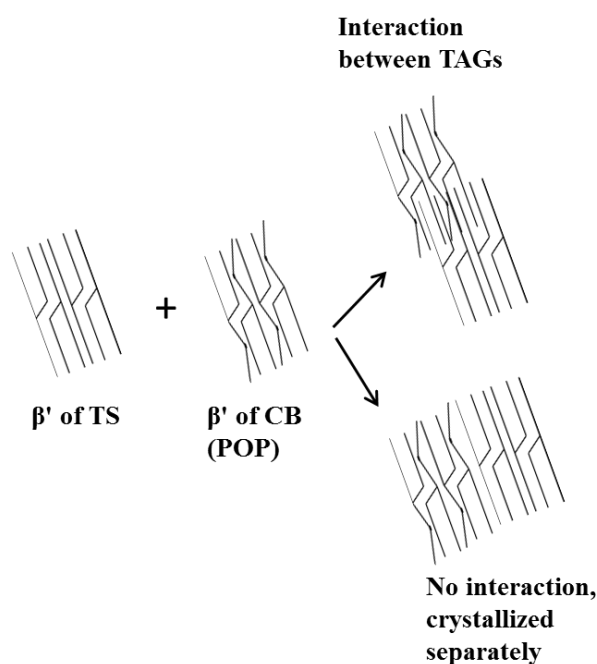


Figure 30: Schematic representation of possible interaction between metastable polymorph of both TS and CB (POP).

In case of blends, interaction between CB and TS is hard to understand due to less information collected from XRD method. Though, we know less miscibility occurred between CB and monosaturated triglyceride (SSS) due to double bond in CB, they could interact in different way with each other, depending upon the composition of TAGs in CB, the cooling

rate (process) used for crystallization form a partial mixture, amount of individual fat in the mixture etc. In schematic above possibility of their interaction is predicted. While drawing the cartoon (Figure 31), it was assumed that only one polymorph is formed in both fats as (β' with tilt angle 70°) and POP was considered as the main TAG component in CB, then there could be either interaction between them i.e. TAGs will try to arrange themselves properly (observed in DSC results of segment 1 and also in XRD) or no interaction, i.e. TAGs will crystallize separately without any interaction (segment 3 in DSC results due to 2 K/minute rate). Therefore, it was hard to specify the exact interaction between these two fats due to complexity in the structure. For understanding more about the precise subcell crystalline structure of fats, miller indices (h,k,l) are required to calculate. This will be an interesting point to follow in near future.

3.3 Study of changes in crystal morphology of CB and TS blends

Polarized light microscopy was used to study the crystal morphology (shape) of pure CB and TS, as it was observed in DSC results that they crystallized with combination of different polymorphs at the rate of 2 K/minute. Also, after mixing these two fats together, the changes occurred in crystal morphology apart from their pure system. In Figure 32, all microscopy images are shown for pure systems and their respective mixtures. Morphology of crystals is usually dependent on the cooling rate used for crystallization and which ultimately derives kinetics of nucleation and crystal growth rate. The slower the rate of growth of crystal surface, higher the probability of surface to be occurred with large surface area (Himawan et al., 2006). Each experiment was performed in three segments similar to process used for DSC measurements. While heating in first segment, it was observed that, in case of mixtures, CB melted earlier at temperature ($\sim 33^\circ\text{C}$); depending on the concentration of CB and TS crystals were surrounded by molten CB. As temperature increased, TS crystals also melted simultaneously however only small amount of crystals melted, which could mean that only small amount of less stable polymorph was present in pure TS. This melting behavior is shown in Image 3 for mixture of TS (40%) + CB (60%). After placing the sample on microscope slide, it looked as a bulk mass, which is shown as a native sample, then after increasing temperature the CB started to melt slowly with respect to the presence of polymorph in the mixture, hence at 39.3°C CB was melted but it was not appeared so clearly, this behavior was also observed in DSC (segment 1; cyan color curve), as there was no specific peak formed at lower temperature to show the melting of CB. At 55°C , the picture

becomes more transparent as the melting of TS has already started, but very slowly. Further increase of two degrees temperature (57.2 °C) the melting process becomes faster, which look like flood, where one polymorph of TS was present in crystal form surrounded by CB and another less stable polymorph of TS in molten form. And at 65 °C, everything was in liquid form. After this segment, the temperature was kept at 70 °C for 5 minutes to be sure of complete melting, and then the crystallization started. In Figure 32, the crystal morphology of all the samples is shown.

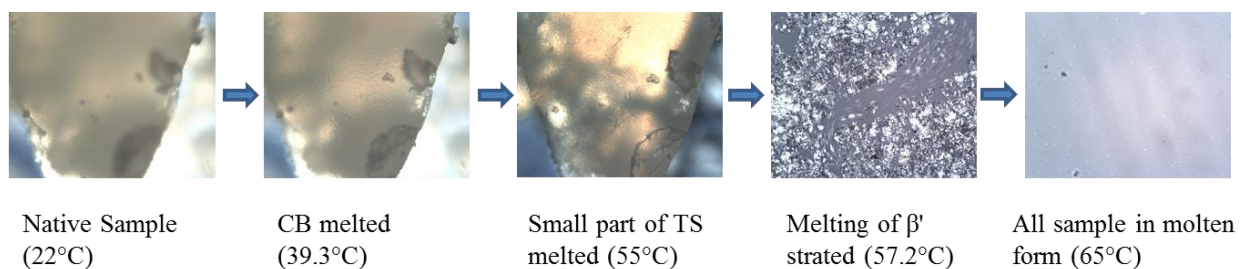
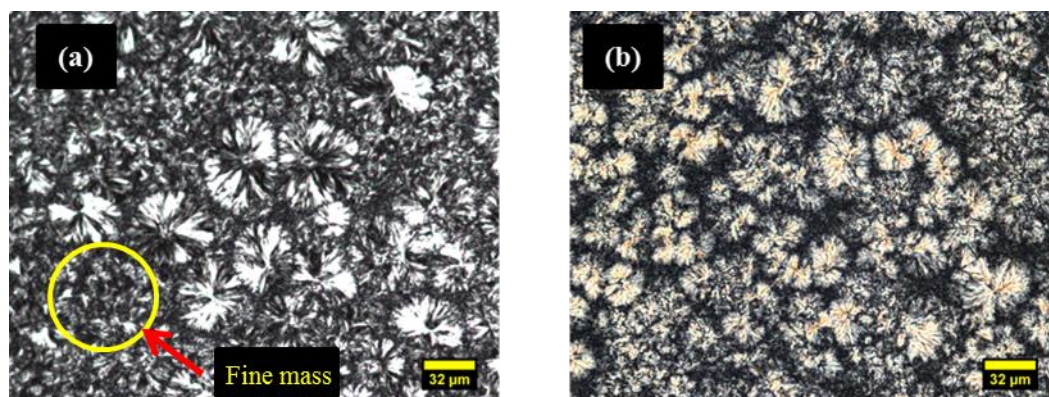
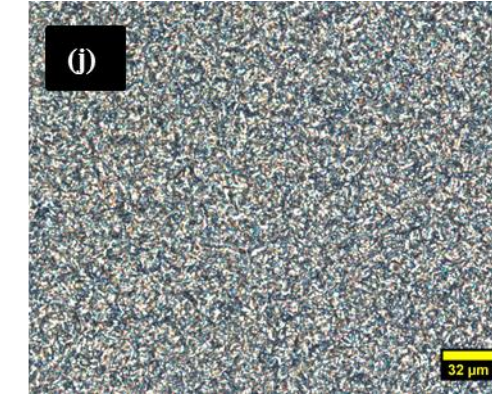
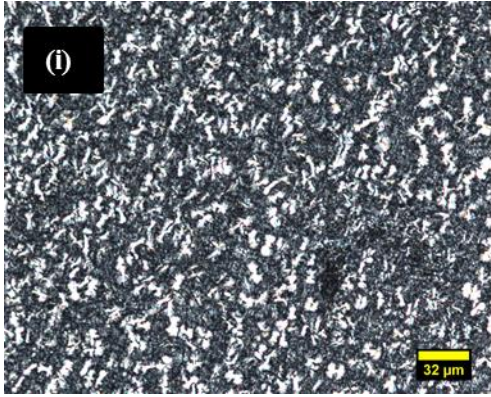
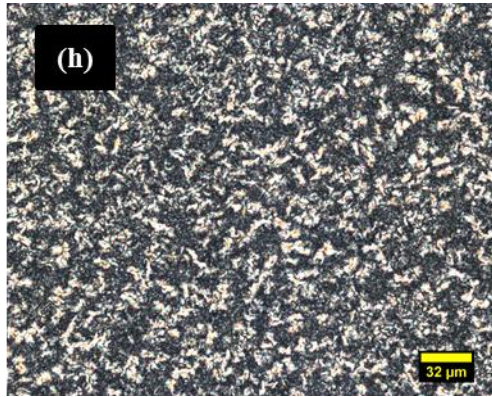
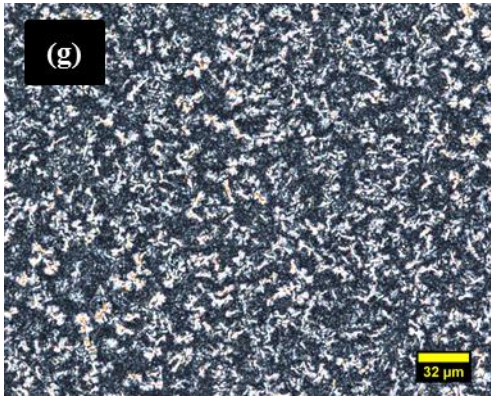
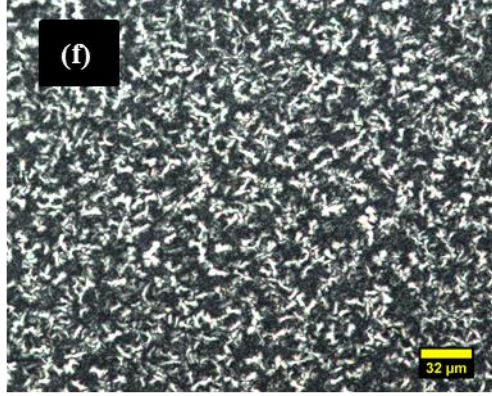
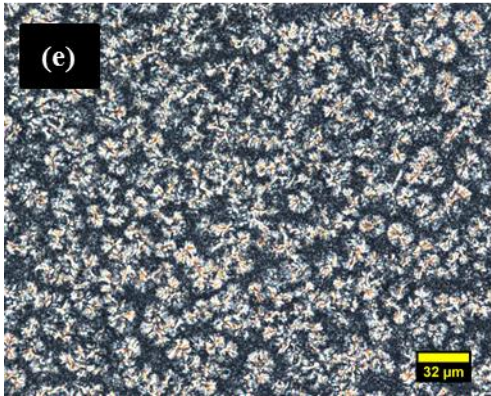
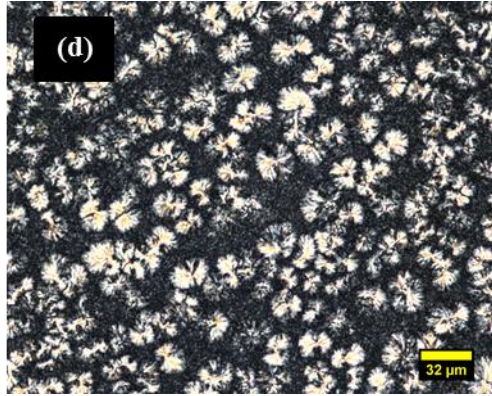
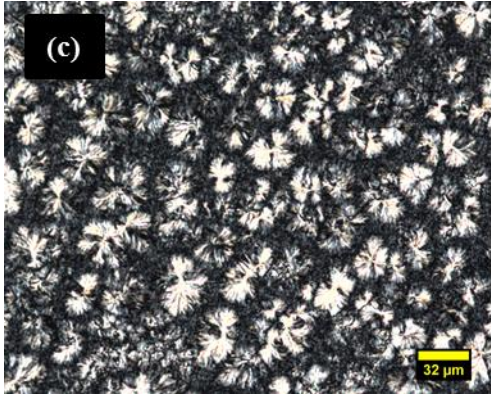


Image 3: The path for melting of crystals in the mixture of TS (40%) + CB (60%).

In image of pure TS (Figure 32 (a)), the mixed crystals with morphology of spherulitic nature and also with fine mass (e.g. shown in yellow circle) was present, this could be because of presence of two polymorph in which one represent the β' (spherical), and another as α (fine mass) (Himawan et al, 2006). These spherulite crystals forms composed of many crystalline ribbons, which grow radially from the center of the nucleus, and those ribbons are usually as needle like shape. As the concentration of CB increased in TS, there was a change observed in crystal morphology in each mixture. In mixture of 10%-wt of CB of TS/CB, the size of crystals become smaller as compared to pure TS, and also the shape of spherulites was distorted. The reason for such behavior is explained by Himawan et al., 2006 in their review paper where they say that this could be due to difference in the driving forces required for the primary and secondary nucleation. According to their study, at low and moderate driving forces, one layer of primary nucleation occurred firstly and afterwards, the layer from secondary nucleation is created (e.g. in case of TS), but at higher driving force, the layer from secondary nucleus started to form simultaneously with the 1st layer. Therefore, the crystal structures did not get appropriate time to arrange themselves in right form and eventually distortions occurred. Hence, possible reason for nucleation of crystals in case of blends that TAGs of CB could promote the higher driving forces, which are required for secondary nucleation. As the concentration of CB increased in TS, more distorted and smaller size crystal formation took place until the 60%-wt TS of TS/CB mixture (i.e. in (c), (d) and (e)).

Furthermore, at 50-50%-wt of TS/CB, the crystal size decreased to broad needle like structure. This behavior of crystal structure was similar until 80%-wt of CB. But in case of 90% of CB, very fine mass was observed. During crystallization of this sample, firstly, the needle like structure was formed and as the temperature decreased further simultaneously the fine mass was started to form. At 10°C it was hard to differentiate between the two crystal morphologies. However, in case of pure CB, the sharp needle like structure formed along with some fine mass which is shown in Figure 31(k). Conversely, Toro-Vazquez et al., 2004 in their study of isothermal crystallization of CB found that below 19 °C, two dimensional crystal formation occurred i.e. disk like structure were formed whereas, above 19 °C, they found three dimensional, i.e. spherical structures. Further they confirmed these observations using ‘Avrami index’. Avrami index indicates the geometry of crystal structure, if the value of exponent is more than 3, then the crystal would be in 3 dimensional and value less than 3 represents 2 dimensional geometry (i.e. disk like in case of CB). Also according to review paper (Himawan et al., 2006); they discussed that needle like structure is because of the β form, although it is often found that the crystal morphology of specific polymorph changes according to the crystallization process. Hence, comparison with DSC results and the crystallization process used in our study shows that morphology of needle like structure crystals were due to formation of α and mixtures of other polymorph.





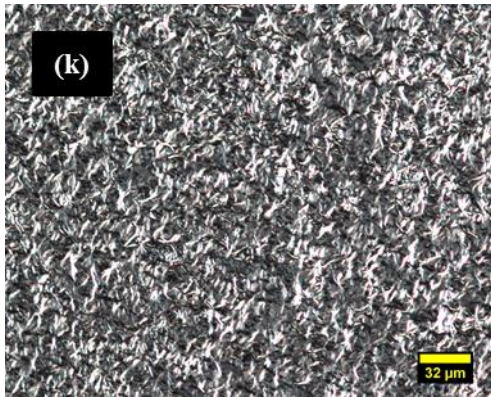


Figure 31: Difference in crystal morphology in case of blends of CB/TS with respect to their concentration in the mixture. The samples are as- (a) Pure TS, (b) TS (90%) +CB (10%), (c) TS (80%) +CB (20%), (d) TS (70%) +CB (30%), (e) TS (60%) +CB (40%), (f) TS (50%) +CB (50%), (g) TS (40%) +CB (60%), (h) TS (30%) +CB (70%), (i) TS (20%) +CB (80%), (j) TS (10%) +CB (90%), (k) Pure CB; (CB- Cocoa Butter; TS-Tristearin; with scale bar of 32μm).

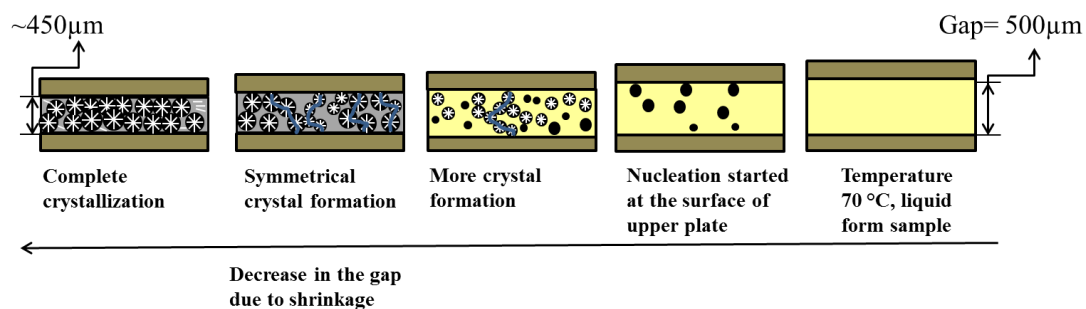
After crystallization process, again the heating of these crystals was carried out to study how the melting of such crystals took place. Firstly, during melting again CB crystals starts to disappear at lower temperature and then the crystals of TS begins to melt, although the solid-solid transition could not be detected precisely.

The results obtained from DSC, XRD and microscopy showed crystallization behavior at static condition, but what would happen on blends of CB and TS when shear is applied to the system while cooling process. Therefore, parallel plate rheometer was used to observe the changes in their rheological properties.

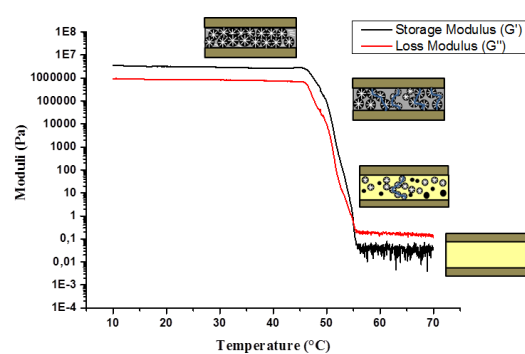
3.4 Analyzing rheological properties of CB and TS during crystallization process

In case of lipid system, crystallization could be taking place via percolation phenomenon. Percolation is a process by which paths are formed through random media. Therefore, during crystallization of fats, crystals could form specific path in the media of molten liquid. In Figure 33 (a), the general scheme of crystals formation during rheology is shown along with the path formation to reach it to lower plate. The co-relation with the rheology result is shown in Figure 33 (b). While drawing this scheme it was assumed that the spherical crystal morphology occurred during crystallization. The cartoon (Figure 32(a)) is showing that sample was in liquid form after placing it on plates with temperature of 70°C. In Figure 32(b) the sample in liquid form is measured as the steady moduli at lower values. The gap between

plates was set to 500 μm . As temperature decreased further, the nucleation (black dots) occurs at upper plate surface due to inhomogeneous temperature distribution between the plates (as only lower plate was attached to the peltier heating/cooling system). Afterwards, the crystal growth occurs with formation of new other crystals (secondary nucleation) in next step and simultaneously gap between the plates was decreasing due to shrinkage of sample. So as the number of crystals increases, the randomly formed crystals could arrange themselves in a path which follows from upper to lower plate (with blue line in Figure 33 (a)), therefore, the increase in modulus observed while measurements (Figure 33 (b)). Further decreased in temperature allows to form more number of crystals which ultimately increases the number of paths from upper to lower plate until they start to overlap with each other. Hence, more increase in modulus observed (Figure 33(b)). But as soon as the temperature decreased again, crystal structures try to overlap (merge) in order to fit in the certain area and therefore the distorted crystals formation occurs (explained in microscopy results as well). After complete crystallization of sample, the moduli values become stable again (Figure 32 (b)).



(a)



(b)

Figure 32: (a) Schematic representation of crystallization of fats during rheology (b) Correlation between the schematic and one result from rheology.

To study the changes in rheological properties during crystallization of fats, the oscillatory shear rheometry was used. The measurements of shear rheometry was depicted in terms of storage modulus (G') and loss modulus (G'') during crystallization of fats. The cooling rate used during measurement was 0.5 K/minute. In Figure 34, the results of all samples are shown. Different colors represents different samples with solid line as storage modulus (G') and dotted line as loss modulus (G''). Storage modulus represents the elastic modulus and loss modulus represents the viscous modulus in the dispersed system which means capacity of storing the energy required for process and loss of energy (energy dissipated as a heat) during the process. So when cooling process started from temperature 70 °C, sample was in liquid form, therefore the loss modulus (G'') was more than storage modulus (G') and as soon as crystallization started (shown in red circle) the storage modulus started to dominate over loss modulus. Another observation corresponding to solidification of sample was, during the crystallization process, steps occurred (shown by arrow in Figure 34) this could be because of the polymorphic transition i.e. 1st stable polymorph starts to crystallize at higher temperature then it gets to transform into another one and therefore steps are formed, similar behavior was also observed during DSC measurement. To explain this behavior in detail, the superimposing of DSC and rheology result for pure TS is shown in Figure 34. The cooling rate used for both process was same. In DSC, firstly, TS was kept at isothermal temperature (70 °C) for about 10 minutes, the distribution of time was selected as like rheology (5 minutes for heating in water bath and 5 minutes of soaking time on rheometer plate, explained in section 2.2 D). However, the caution to be considered while comparing these two results together due to parameters, such as differences in volume of the sample, heating system used in both cases were different, and different equipment design, this somehow must have affected the final result.

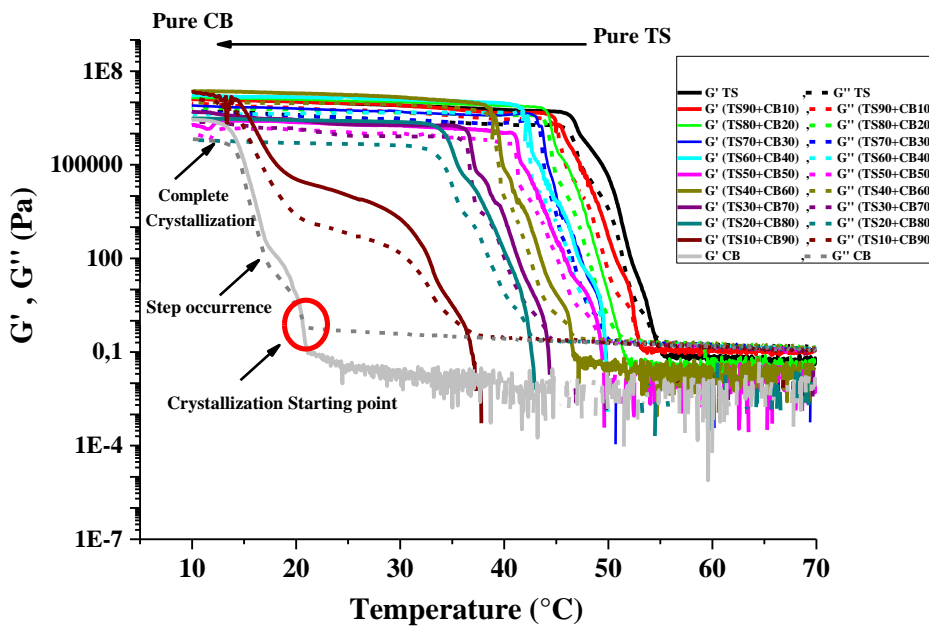


Figure 33: Graphical representation of moduli vs. temperature in which the changes in moduli after addition of CB in TS during crystallization process is shown. (G' –Storage Modulus, G'' -Loss modulus; CB-Cocoa Butter, TS- Tristearin).

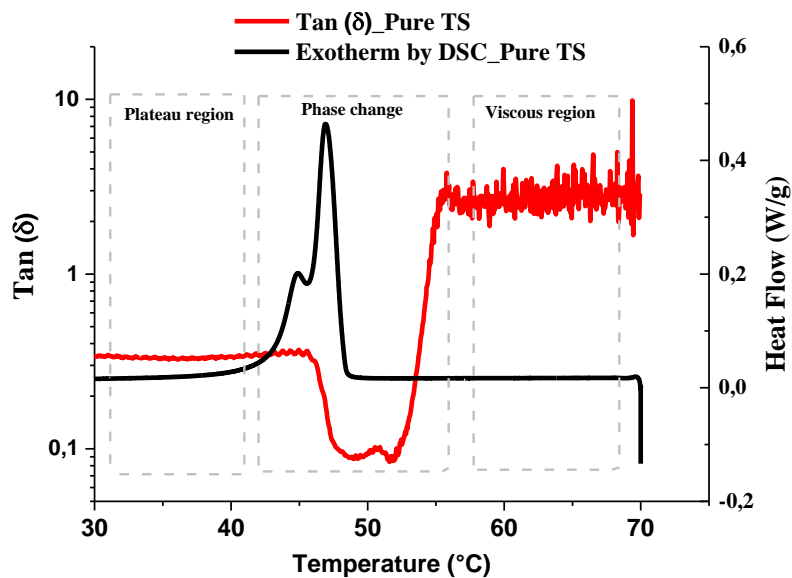


Figure 34: Co-relation between rheology and DSC result for pure TS sample to understand the change in viscoelastic properties during crystallization process.

In Figure 35, the graph between $\tan(\delta)$ (left y-axis), which is the ratio of G'' and G' illustrates the change in viscoelastic properties of lipid systems with respect to applied temperature. In this case, pure TS was in liquid form at 70 °C, hence the phase angle (δ) is at

its highest i.e. 90° , which is shown as viscous region (Figure 35). As soon as the nucleation started, the phase angle decreased to very low point, this indicated that there was a phase change from liquid to solid, similarly, in thermogram (black curve, heat flow scale on right y-axis), the peak increased drastically. In exotherm, the incomplete crystal growth of one polymorph occurred, and another polymorph started to form simultaneously (could be because of higher nucleation driving force), which was detected as a shoulder peak, hence the inhomogeneous crystal formation occurred. Comparable observation was obtained in rheogram as there was also formation of another shoulder peak. The heat released during crystal growth process resulted in formation of a peak in terms of DSC and in case of rheogram the peak was observed due to change in texture (Toro-Vazquez et al., 2002). Afterwards, complete crystal growth takes place, which is shown as a plateau region. Similar results were obtained in case of pure CB also (Figure 36). Only difference was that both DSC result and rheology result of CB appeared exactly on similar position, whereas, in case of pure TS, the exotherm peak was shifted towards, less temperature than rheology result. This was because of either the inhomogeneous temperature between two parallel plates or due to rupture in sample structure due to applied amplitude. Since TS is less elastic than CB, TS started to crystallize at higher temperature.

Toro-Vazquez (2004) also observed the similar behavior during their experiment with pure CB; however, they carried out isothermal crystallization at (18°C , 18.5°C , 19°C and 22°C) for observing the polymorph transition. In pure CB, they observed that three peaks as polymorph α , β' , β respectively, with plateau region in between and then phase angle was decreased to 0° after complete crystallization, whereas, in our study the phase angle was not completely at 0° . Also with palm stearin and sesame oil blend only one peak was observed in both DSC and rheology instead of two peaks observed for pure TS in our study, because there was only one polymorph formed during crystallization process (Toro-Vazquez et al., 2002). Similar observations were obtained in each blend of CB and TS.

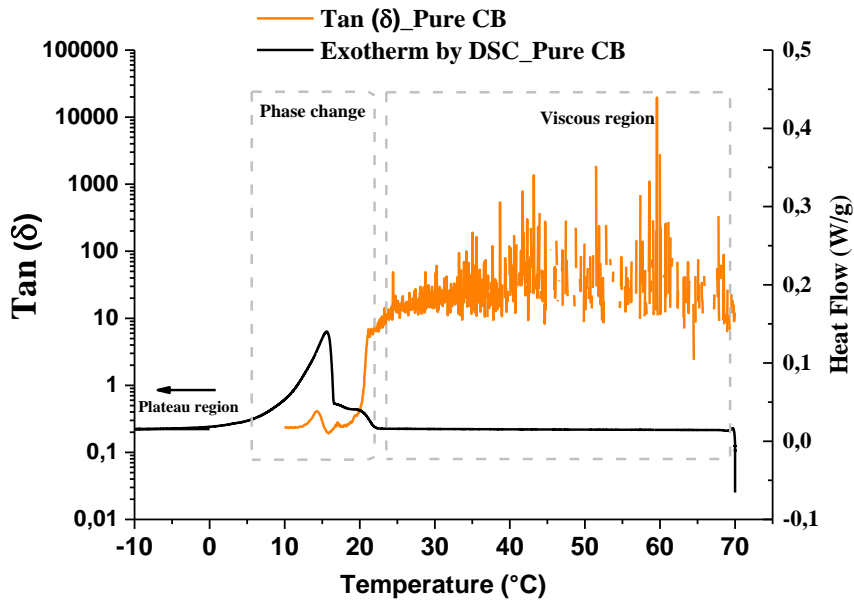


Figure 35: Co-relation between rheology and DSC result for pure CB sample to understand the change in viscoelastic properties during crystallization process.

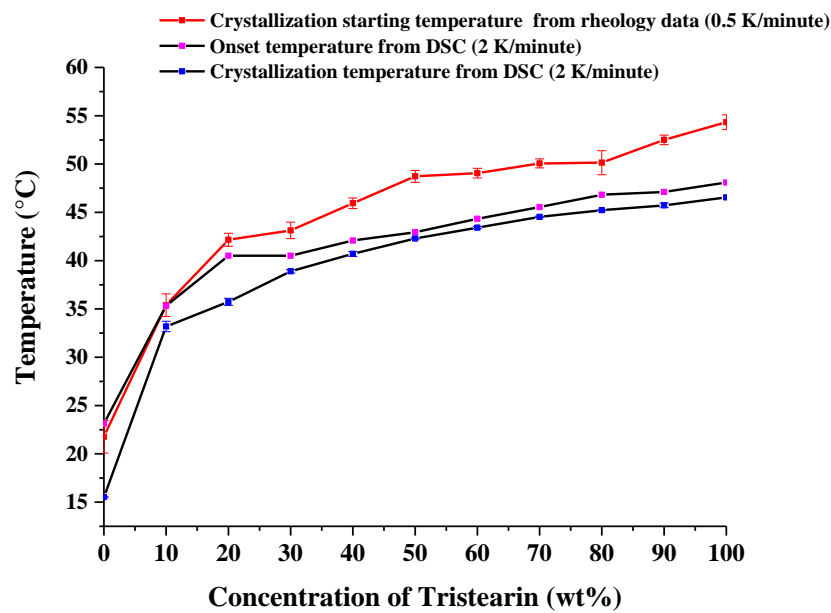


Figure 36: Graphical representation of change in crystallization temperature during rheology experiment.

Another observation from Figure 34, that there was a shift in starting temperature of crystallization taking place after addition of CB in TS. The evaluation of this data was carried

out in origin software and is plotted in Figure 37 along with the results obtained from DSC (onset temperature and crystallization temperature of CB/TS mixtures). It is a graphical representation between changes in crystallization temperature with respect to the concentration of TS. As the concentration of CB increased the crystallization temperature started to decrease further, which was also observed in case of DSC results (segment 2). TS started to crystallize at higher temperature as it is a monosaturated triglyceride and also because of inhomogeneous temperature distribution between upper and lower plate (also described in fig. 35) and therefore, it acted as a nucleus for TAGs components of CB and hence they arranged themselves according to the crystal structure of TS. Also, only at 10% of TS in CB, the shift in starting of crystallization was much greater as compared to pure CB; this behavior explained that TS started to dominate over CB even at fewer amounts. Similar behavior was obtained in case of DSC measurement. As rheology is a technique which shows mechanical properties, only one crystallization starting temperature was seen in blends instead of two different peaks detected during DSC measurements.

3.5 Effect of tempering on polymorph formation

Tempering process helps to form more stable polymorph during cooling of fats. However, only proper tempering process encourages forming the nuclei of the stable polymorph first and then it acts as seed crystal for rest of the liquid fat. Tempering is dependent on the stirring speed, accurate temperature, time duration for formation of proper nuclei and less amount of humidity (Beckett, S. T. 2000). In this experiment, two methods were used for tempering process (explained in material and method section). Only pure CB and TS were considered for tempering to find the optimize parameters for achieving most stable polymorphs.

3.5.1 Effect of tempering on pure CB

In Figure 38, the results of tempering were obtained by using constant climate chamber and by water bath. Only first melting segment is considered in this figure because after heating CB at 70 °C, it destroyed the previous crystal memory and hence it showed the similar exotherm as it was observed in previous cases (segment 2). Hence, our DSC results (segment 1) predicted that without tempering of CB, β_1' (as main peak) and β_2 (as shoulder peak) polymorphic forms occurred, but if we compare this result to the endotherm detected in DSC from tempering at 27 °C (which was carried out in closed water bath system), the formation of most required (in confectionery applications) polymorph β_2 (Form V) was achieved in large amount as it was not the case in other tempering results of pure CB. Another process

conditions applied on pure CB in 4 different steps and the DSC measurement detected the endotherm (CB_tempered_#1), which illustrated that there were occurrence of three most stable polymorph as β_1' , β_2 , β_1 respectively, which are as shown in fig 38. This DSC measurement was done after 7.30 hours of cooling at room temperature, therefore it was crystallized in three polymorphs, but if the more time could have been provided for cooling process, there could be a possibility of formation of only one polymorph instead of coexistence of three. The comparison between two tempering process one at 27°C and another with 4 different steps shows us that even with no shear is applied during tempering, the tempering at 27 °C promotes the nucleation of β_2 crystals which then acted as a seed for rest of the molten liquid. Whereas in case of tempering at 32 °C (last step in CB_tempered_#1), the less amount of solid fat is present, therefore, the kinetic energy of crystals would be higher and hence resulting in more randomization of crystals. This eventually increases in entropy of the system and so leading to decrease in Gibbs free energy. In statistical mechanics, the Boltzmann factor is denoted as.

$$\text{Boltzmann factor} - \exp^{-\frac{E}{kT}}$$

So in case of tempering at 32 °C, Boltzmann factor would be higher as compared to the tempering at 27 °C. Therefore, the probability distribution of these polymorphs (which formed at tempering 32 °C) to attain at this state will be higher as compared to polymorph occurred at 27 °C tempering.

However, in industrial confectionary applications the tempering machine is used for forming stable polymorph in CB with the same temperature conditions used in case of CB_tempered_1# results, but the induction time required for nucleation and fast crystal growth would be optimized by using stirring process, with the speed of about 3000 to 8000 s⁻¹ (Beckett, S. T. 2000). This speed limit is set with respect to the size of motor for rotator and heat generated during mixing. If the heat generated becomes more, then the stable polymorph will also melt which will affect the ultimate quality of product. Hence, to study the effect of stirring on polymorph formation, the next experiment was performed and the data is shown as a blue curve in Figure 38. From the results it has been cleared that with these parameters poorly tempered CB was obtained. This could be because of the nucleus formation of less stable polymorph and there would be so any reasons such as-1) the speed of magnetic stirrer was same in all sets of temperature, as at 26 °C, the CB should be sheared at higher speed for stable formation polymorph 2) usually newly formed crystals are smaller in size, which could easily be melted if the heat was increased due to the speed, this could occur at last step (32

°C). Hence, proper set of temperature, speed and time for cooling should be provided for good tempered CB.

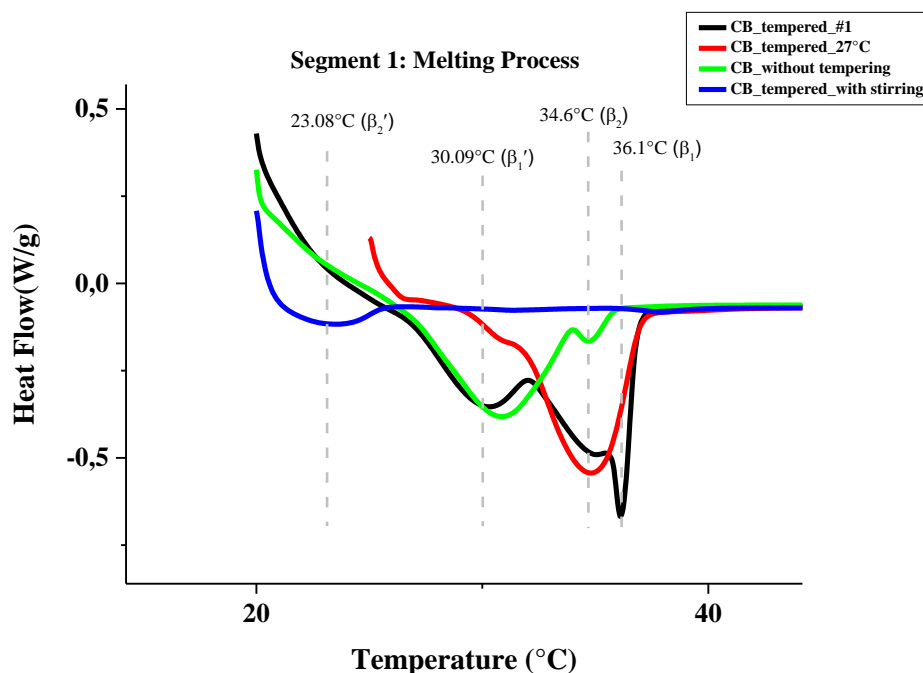


Figure 37: Comparison of polymorphism in tempered and non-tempered CB; (CB_tempered_#1- 60 °C for 15 hours, 30°C for 2 hours, 26 °C for 1 hour, 32°C for 2hours; ‘CB_tempered_with stirring’, with same parameter as in CB_tempered_#1 along with 350 rpm speed).

3.5.2 Effect of tempering on pure TS

In Figure 39, the results obtained after DSC of tempered TS is shown. Only 1st melting was considered as after melting at 70°C after melting segment, it gave the same crystallization peak as it was before, which is shown in case of segment 2. Pure TS was tempered at three different conditions to observe the change in polymorph formation. Following observations made from measurements.

- a) In case of non-tempered TS, which were stored at room temperature (~22°C) for overnight before DSC, the solid-solid transition was seen due to polymorph transition, this behaviour was also observed during tempering at 27°C with little shift to higher temperature with decreased peak height and also the endothermic peak shifted to higher temperature. This shows that the thermodynamic stability increased due to tempering at 27°C, this could also mean that the spacing becomes very strong for this form of polymorph and hence melting occurred at higher temperature. There was also

formation of shoulder peak near to the melting peak, which could be because of either impurity in the sample or presence of another polymorph in the system.

- b) When TS was tempered at 60°C for 20 hours, which is slightly less than the melting temperature of β' polymorph, the solid-solid transition curved diminished this could be because TS acquired much time to form β' polymorph directly from liquid melt. However, there was also presence of shoulder peak because of either impurity or another trace of polymorph. Another observation was, the peak become much broader as compared to without tempered TS and tempering at 27°C, and also it shifted to higher temperature.
- c) Sample with 'TS_tempered_#1' in figure 39, was prepared in 4 segments which is explained in material and method section. With these process conditions, again only one polymorph was formed from liquid melt as there is no sign of solid-solid transition exotherm. Also, the shoulder peaks now vanished, which means only one polymorph was formed as controlled cooling took place.

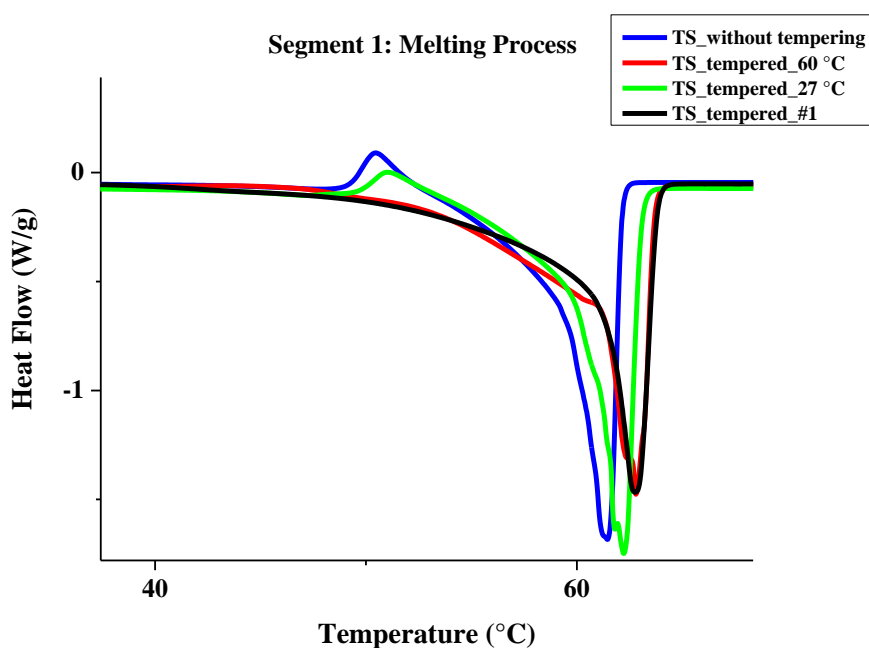


Figure 38: Comparison of polymorphism in tempered and non-tempered TS; (CB_tempered_#1- 60 °C for 15 hours, 30°C for 2 hours, 26 °C for 1 hour, 32°C for 2hours).

Chapter 4

Conclusion

Fundamental studies of thermal, physical and mechanical properties of individual fats and oils and their respective blends ultimately help to optimize the process for making good food products. Therefore, it is necessary to investigate the changes that occur during mixing two fats or fat/oil together on their physicochemical properties. In this work we find that in case of CB and TS blends, melting temperature and crystallization temperature is decreasing in TS due to presence of oleic acid in CB, whereas, CB does not show any significant change in its thermal properties. On the other hand, the blends of CB and CO form a eutectic mixture at 60% and 70% -wt of CO because of the closer melting temperature of both systems. Therefore, it could be concluded that monounsaturated TAGs present in CB has a tendency to form new molecular compound when it interacts with mixed short chained TAGs (CO) but with long chain monosaturated TAG (TS), it needs time to interact properly. Also thermodynamically less stable polymorph is formed in pure system due to addition of other fats and oils in larger amounts. Furthermore, the crystal morphology of pure CB and TS changes after mixing these two fats together. In Pure TS, spherical shape and some small size like fine mass crystal structure occurred ($\beta'+\alpha$) and in pure CB, a needle like structure is formed along with fine mass. All mixtures show the change in crystal morphology according to the concentration of CB and TS in it. However, XRD could not provide specific conclusion in case of blends of CB and TS. With this limited information from XRD data it is hard to conclude the specific structure formation in case of mixtures. Similarly, rheology results show that onset crystallization temperature decreases after addition of CB to TS along with inter-polymorphic transition in between. Hence, due to different composition of TAGs in CB, it is hard to form only one polymorph with 2 K/minute rate; however, further decrease in the rate will help to form one polymorph instead of mixtures of polymorph, which will ultimately increase the thermodynamic stability. Moreover, the tempering would also help to form more stable polymorph in case of pure TS and CB.

Chapter 5

Outlook

In future, the focus will be on the tempering process of individual fats and oil to determine the optimized procedure for obtaining most stable polymorph, similarly also for their respective blends. In addition, determination of the precise crystal structure of pure CB and TS can be done with the help of powder cell XRD method. Next focus will be on the fitting of phase diagram that is obtained from DSC results with the help of Margule's equation and kinetics involved in fat/oil crystallization process.

Chapter 6

References

- Abdulkarim, S. M., Myat, M. W., & Ghazali, H. M. (2010):** Sensory and physicochemical qualities of palm olein and sesame seed oil blends during frying of banana chips. *Journal of Agricultural Science*, 2, 18e29.
- Beccard S., (2016):** Published in private communication.
- Beckett, S. T. (2000):** *The Science of Chocolate*. Royal Society of Chemistry, Cambridge, pp. 85-103.
- Bruin, S. (1999):** Fluid phase equilibria. 160-657.
- Davis, T.R., and Dimick, P.S. (1989):** Crystals formed during Cocoa Butter solidification. *J. Am. Oil Chem. Soc.* 66:1488–1493.
- Davis, T.R., and Dimick, P.S. (1989):** Lipid composition of high-melting seed crystals formed during Cocoa Butter solidification. *Ibid.* 66:1494–1498.
- Fernandes, V.A., Müller, A., and Sandoval, A. (2013):** Thermal, structural and rheological characteristics of dark chocolate with different compositions. *Journal of Food Engineering* 116 .97–108.
- Feuge, R.O., Landmann W., Mitchman D. and Lovegren N.V. (1962):** Tempering triglycerides by mechanical working. *J.Am.Oil Chem. Soc.* 39:310-313.
- Hagemann, J.W., In: Garti, N., Sato, K., editors. (1988):** Crystallization and polymorphism of fats and fatty acids. New York: Marcel Dekker; p. 9.
- Himawan, C., Starov V.M., Stapley A.G.F. (2006):** Thermodynamic and kinetics of fat crystallization. *Advances in Colloid and Interface Science* 122, 3-33.
- Jahrulu, M. H. A., Zaidul, I. S. M., Norulaini, N.A. N., Sahena, F., et al. (2014):** Characterization of crystallization and melting profiles of blends of mango seed fat and palm oil mid-fraction as cocoa butter replacers using differential scanning calorimetry and pulse nuclear magnetic resonance. *Food Res. Int.* 55, 103-109.
- Loisel, C., Keller G., Lecq G., Bourgaux C., and Ollivon M. (1998):** Phase transition and polymorphism of Cocoa Butter. *J. Am. Oil Chem. Soc.*, Vol. 75, no.4.
- McCabe, W.L., Smith, J.C., and Harriott, P. (2005):** Unit operations of chemical engineering. 7th ed. pp. 929-943.
- MacNaughtan, W., Farhat, I.A., Himawan, C., Starov, V.M., and Stapley, A.G.F. (2006):** A Differential scanning calorimetry study of the crystallization kinetics of Tristearin-Tripalmitin mixtures. *J. Am. Oil Chem. Soc.*, Vol. 83, no. 1.
- Mayama, H. (2009):** Blooming theory of tristearin *Soft Matter* 5 856–9.
- Mazzanti, G., Guthrie, S.E., Sirota, E.B., Marangoni, A.G., and IDziak, S.H.J. (2003):** Novel shear-induced phase in Cocoa Butter. *Ibid.* 4:409-411.
- Nguyen, T.K. (2009):** *Chemical Engineering Thermodynamics II*.
- O'Brien, R. (2009):** *Fats and oils formulating and processing for applications*. 3rd ed. Taylor and Francis Group.
- Oldenbourg, R. (2013):** *Polarized Light Microscopy: Principles and practice*. Cold Spring Harb Protoc.

- Quinones-Munoz, T., Gallegos-Infante, J.A., et al. (2010):** Mixing and tempering effect on the rheological and particle size properties of dark chocolate. *Journal of Food*. Vol. 9, no. 2, 109–113.
- Rothkopf, I. and Danzl, W. (2015):** Changes in chocolate crystallization are influenced by type and amount of introduced filling lipids, *Eur. J. Lipid Sci. Technol.* 117, 1714-1721.
- Sato K., (1999):** Solidification and phase transformation behavior of food fats: a review. *Fett/lipid*, 101, 467-474.
- Sonwai, S. Mackley M.R. (2006):** The effect of shear on the crystallization of Cocoa Butter. *J. Am. Oil Chem. Soc.*, Vol.83, no.7.
- Tan, C.P., and Che Man, Y.B., (2001):** Differential scanning calorimetric analysis of palm oil, palm oil based products and coconut oil: effects of scanning rate variation. *Food Chemistry* 76. 89–102.
- Toro-Vazquez, J.F., Perez-Martinez, D., et al. (2004):** Rheometry and polymorphism of Cocoa Butter during crystallization under static and stirring conditions. *J. Am. Oil Chem. Soc.* Vol. 81, no. 2.
- Toro-Vazquez, J.F., Herrera-Coronado, V. et al. (2002):** Induction time of crystallization in vegetable oils, comparative measurements by Differential Scanning Calorimetry and Diffusive Light Scattering. *J. Food Sci.* 67:1057-1065.
- Vilgis, T. (2015):** Soft matter food physics-the physics of food and cooking. *Rep. Prog. Phys.* 78. 82pp.
- Wille, R.L., Lutton, E.S. (1966):** Polymorphism of Cocoa Butter. *J. Am. Oil Chem. Soc.* 43:491-496.
- Windbergs, M., Strachan C.J. and Kleinebudde P. (2009):** Investigating the principles of recrystallization from glyceride melts. *AAPS PharmaSciTech*, Vol. 10, no.4.
- Wim H. (2016):** Basic X-ray scattering for soft matter. 1st ed. pp. 4-6.

Acknowledgements

First of all I would like to thank Prof. Dr. Thomas Vilgis for providing me opportunity to carry out Master's thesis. Thanks for your support, your trust and encouragement. You're a great mentor!

Thank you, Prof. Dr. Kremer, for allowing me to carry this work at Max Planck Institute of Polymer Research

I would like to express my deepest gratitude towards Birgitta for supervising my work with patience, I really enjoyed all those discussions with you and they really helped me a lot in understanding the topic well.

Thank you so much Steffen, for helping me out with all doubts that I had always and also your support and willingness to help me during my entire work.

Thanks Ashutosh, Hannah, Sarah and all group members.

I would also like to thank all Technical Assistants for their help in carrying out experiments.

I also would like to thank Prof. Dr. Staudt for being my internal supervisor during my research work.

Last but not least, I would like to thank my family members back home for their constant moral and financial support without which it would be impossible to carry out my studies. I thank you all!